Chalcogenide Synthesis

International Edition: DOI: 10.1002/anie.201507736
German Edition: DOI: 10.1002/ange.201507736

Synthesis of Crystalline Chalcogenides in Ionic Liquids

*Silke Santner, Johanna Heine, and Stefanie Dehnen**

Keywords:
chalcogenides · chalcogens · ionic liquids · ionothermal synthesis · structures and properties

Dedicated to Professor Bernd Harbrecht on the occasion of his 65th birthday

Crystalline chalcogenides belong to the most promising class of materials. In addition to dense solid-state structures, they may form molecular cluster arrangements and networks with high porosity, as in the so-called "zeotype" chalcogenidometalates. The high structural diversity comes along with interesting physical properties such as semi-/photoconductivity, ion transport capability, molecular trapping potential, as well as chemical and catalytic activity. The great interest in the development of new and tailored chalcogenides has provoked a continuous search for new and better synthesis strategies over the years. The trend has clearly been towards lower temperatures for both economic and ecological reasons as well as for better reaction control. This led to the application of ionic liquids as a designer-like medium for materials synthesis. In this Review, we summarize recent developments and present a survey of different chalcogenide families along with their properties.

From the Contents

1. Introduction

1.1. Chalcogenides—From Basic Research to Application

The application of chalcogenides in a diversity of technical fields is very promising due to their suitable optoelectronic, electrochemical, and structural properties.[1] In particular, crystalline chalcogenide frameworks have received attention because of the combination of specific structural features with semiconductivity.[2,3] This is particularly the case for porous chalcogenides,[4–8] as these comprise both high surface areas and physical or physicochemical properties that enable their applicability in optoelectronic devices,[3b,5] photocatalysis,[2b,6] fast ionic conduction,[2a,7] and ion exchange.[8] Of course, the specific functionalities are essentially dependent on the framework structures, which are likewise related to the elemental combination.[3a,5a]

A very attractive field of contemporary materials research is thus the generation of new functional crystalline chalcogenides with novel compositions and structures, which includes the development of innovative synthesis methods. It should be mentioned that noncrystalline or microcrystalline chalcogenide materials are also targeted currently by a variety of different synthetic approaches, which will, however, not be the subject of this Review as they have been reviewed extensively elsewhere.[9a]

1.2. Traditional Synthesis Routes

Traditionally, crystalline chalcogenides have been assembled by high-temperature routes, which usually lead to the formation of dense solid-state structures. Most of the syntheses that have addressed the formation of open-framework chalcogenide architectures were so far carried out under elevated temperature, by reactions in polychalcogenide fluxes, as direct replacements for the solid-state techniques,[9b,10] or by hydrothermal or solvothermal reactions.[4d,11,12] The latter were predominantly realized as "one-pot" syntheses, in which the composition and topology were determined by careful selection of the elemental sources.[13] However, such reactions possess a high degree of serendipity in terms of the topologies, whereas better controllable, stepwise reactions involving transformations of identified phases to subtly tune the product properties are comparatively rare.[14] An example is the single-crystal-to-single-crystal (SCSC) transformation.[15,16]

Ambient temperature syntheses are highly desired for even better control of the reaction and these will further affect and vary the product spectrum. Such syntheses additionally comply with contemporary ecological and economic issues. Despite this, syntheses at room temperature, usually performed in protic solvents such as water or alcohols, have remained rare.[17] Usually, synthetic approaches that are carried out in solution produce solvates, and are thus potentially useless for technical applications. Syntheses in solvent-free environments seem to be a most promising route for the generation of solvent-free crystalline chalcogenides, which are advantageous or even necessary, for example, for electrochemical applications, which has led to an enormous amount of research activity into this direction.

1.3. New Synthetic Approaches

Increasing interest in the employment of ionic liquids for the synthesis of crystalline chalcogenides has become noticeable. In particular, reactions under so-called "ionothermal" conditions, which will be detailed in Section 2, have attracted attention.[11] Another related technique that was recently introduced is the "surfactant-thermal" method, which makes

[*] M. Sc. S. Santner, Dr. J. Heine, Prof. Dr. S. Dehnen
Fachbereich Chemie und Wissenschaftliches Zentrum für Materialwissenschaften, Philipps-Universität Marburg
Hans-Meerwein-Strasse, 35032 Marburg (Germany)
E-mail: dehnen@chemie.uni-marburg.de
Homepage: http://www.uni-marburg.de/fb15/ag-dehnen

use of the specific properties of surfactants, such as poly(-vinylpyrrolidone) (PVP), poly(ethylene glycol)-400 (PEG-400), or 1-hexadecyl-3-methylimidazolium chloride ($[C_{16}C_1im]Cl$), at elevated temperatures.[18] In this way, compounds such as $[NH_4]_8[Mn_2As_4S_{16}]$[19] and $[N_2H_4]_2$-$[Mn_3Sb_4S_8(\mu_3\text{-}OH)_2]$[20] were prepared that could not be accessed by traditional routes. A completely solvent-free method for the preparation of crystalline chalcogenides is the mechanochemical approach. This method is especially useful for compounds with extremely high melting points, such as lanthanide chalcogenides.[21]

2. Ionothermal Syntheses

2.1. A Brief History of Ionothermal Syntheses

The term "ionic liquid" (IL) usually describes a saltlike compound which is liquid under ambient conditions (room-temperature ionic liquid, RTIL) or, more generally, which melts below 100 °C (near-room-temperature ionic liquid).[22] A representative historical example of an ionic liquid is ethylammonium nitrate $[EtH_3N][NO_3]$, which was reported by Walden in 1914 to melt at 12.8 °C.[23] In the meantime, more than a thousand ionic liquids have been produced and published, and many of them can be purchased from chemical companies.[22,24,25] The increasing attraction in using ionic liquids is due to their excellent solvating properties, which is characterized by the ability to dissolve a large variety of materials as a result of the specific combination of cations and anions within the "salt", as well as their negligible vapor pressure, high thermal stability, and a wide liquidus range. Contemporary ionic liquids resemble designer chemicals and are continuously developed and improved both in academia and in industry. Today, at least one of the ions is usually organic, which greatly affects the desired low tendency to assemble into solid structures. Recently, the properties and application of ionic liquid mixtures have also been actively discussed.[26]

Ionothermal reactions, in particular, are defined as reactions in ionic liquids that are performed under elevated temperature in sealed systems. In this way, such reactions are similar to solvothermal techniques, although without the generation of a comparably high vapor pressure and thus accordingly not reaching supercritical conditions. Typically, temperatures up to 200 °C are applied, which allows the use of ionic liquids that are not necessarily liquid below 100 °C.[27,28] In these reactions, ionic liquids can act as both the solvent and potential template, namely, the structure-directing agent.

This technique was introduced in 2004 for zeolite syntheses in eutectic mixtures of 1-ethyl-3-methylimidazolium bromide and urea/choline chloride.[11] Its advantage over traditional hydrothermal procedures was put down to the absence of the common competition between the solvent and a template for interaction with the growing solid. Hence, the growing crystal structure benefits from improved templating. This holds in particular for the targeted synthesis of porous crystalline materials. So far, ionothermal techniques have been applied mainly in the synthesis of oxidic materials, in particular of zeolites, metal–organic frameworks[29] and nanomaterials.[30] The application of this technique for the preparation of crystalline chalcogenides, in contrast, is still at its beginning.[31]

2.2. Synthesis of Chalcogen Compounds by the Ionothermal Approach

In the following, we will provide an overview of all the crystalline chalcogen compounds that have so far been obtained from ionic liquids—with the vast majority of them being synthesized under ionothermal conditions. Section 3 deals with chalcogenides, thus with compounds that comprise chalcogen atoms in a negative (average) formal oxidation state. These appear either as salts with polychalcogenido-(semi)metalate anions, or as salts with polycationic metal-chalcogen aggregates. In Section 4 we will shed light on chalcogen compounds with formally neutral or even oxidized chalcogen atoms. A summary of specific properties is also given.

Although all of the compounds presented herein were, in general, synthesized in ionic liquids, the ionic liquid used and the reaction conditions can differ over a wide range. Scheme 1 summarizes all the parameters that can be, and have been, varied during the formation of crystalline chalcogenides in ionic liquids. Scheme 2 summarizes all the cations and anions that have so far been used in the formation of the reported ionic liquids. Notably, all the syntheses have so far been

Silke Santner received her BSc in 2010 and her MSc in 2013 from Philipps University of Marburg, the latter with a thesis on the reactivity of chalcogenidometalates in protic solvents and ionic liquids under the supervision of Stefanie Dehnen. She is currently carrying out PhD research, working on a project dealing with ionothermal syntheses of chalcogenidometalates in the Dehnen group.

Johanna Heine obtained her diploma from Philipps University of Marburg in 2008 and finished her PhD in 2011 under the supervision of Stefanie Dehnen. She then carried out postdoctoral research in the group of Klaus Müller-Buschbaum at the Julius Maximilian University of Würzburg (2012–2013), where she investigated the synthesis and luminescent properties of lanthanide-containing coordination polymers. In 2013, she returned to Marburg for independent research on hybrid compounds based on halogenido metalates.

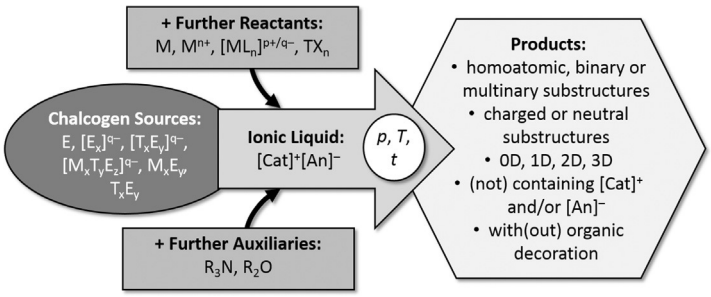

Scheme 1. General synthetic approach for the formation of crystalline chalcogen compounds in ionic liquids, outlining all the parameters that can be varied. The auxiliaries do not necessarily need to be part of the desired products; they instead help to trigger network formation or destruction. In most known cases known, E = Se. $[Cat]^+$ = cation, $[An]^-$ = anion.

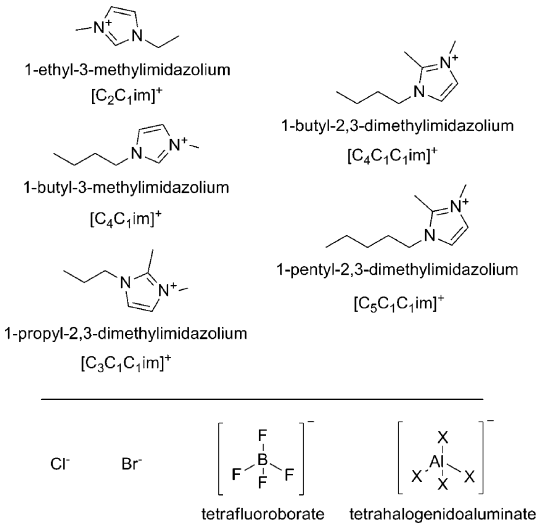

Scheme 2. Survey of the cations (top) and anions (bottom) that have been combined in the ionic liquids used for the generation of chalcogen compounds, along with the corresponding abbreviations. The chain lengths of the substituents at the 1-, 2-, and 3-positions of the imidazole ring will be denoted by parameters *m*, *n*, and *o*, respectively, in $[C_mC_nC_oim]^+$ cations. If only two substituents are given, these refer to organic groups in the 1- and 3-positions.

performed using ionic liquids that are based on imidazolium cations. This is due to the necessity of the ionic liquid to have a sufficiently high polarity to dissolve the precursors and to allow for smooth crystallization of the products. However, it is not ruled out that further combinations of cations and anions will work as well, which has to be explored in future work.

Stefanie Dehnen obtained her diploma in 1993 and her PhD in 1996 from the University of Karlsruhe (KIT) with Dieter Fenske. After a postdoctoral stay with Reinhart Ahlrichs (1997), she completed her Habilitation in Inorganic Chemistry in 2004. In the same year, she was awarded the Wöhler Young Scientists Award from the German Chemical Society. Since 2006 she has been Professor of Inorganic Chemistry at Philipps University of Marburg and Director of the Scientific Center of Materials Science, where she was Executive Director from 2012 to 2014. She is currently a member of the Board of the Division for Inorganic Chemistry at the GDCh.

3. Crystalline Chalcogenides from Ionic Liquids

Chalcogenides may be classified in many different ways. In the following, we will classify the compounds by the nature of their main substructures. In all of the compounds presented herein, the chalcogen atoms are part of complex architectures. Binary or multinary compounds with isolated monochalcogenide (E^{2-}) anions as the crystalline bulk material will not be part of the discussion, as none of the published examples were obtained from syntheses in ionic liquids.

3.1. Polyanionic Chalcogenides

Most of the known complex chalcogenide compounds comprise polyanionic substructures. These appear either as molecular aggregates ("zero-dimensional", 0D), as strands (1D), layers (2D), or three-dimensional networks (3D). Despite the structural diversity of polyanionic chalcogenide substructures, several structural motifs seem to be privileged over others, such that they are observed in many of the phases in various compositions and topological arrangements—this is especially the case with the large number of Group 14 chalcogenide networks, most of which have been selenides so far. The most common motifs will be briefly introduced in the next section.

3.1.1. Predominant Structural Motifs

Common secondary building units (SBUs, Figure 1) are the $[ME_4]$ tetrahedron (TD), the $[M_3E_9]$ defect-adamantane structure (d-AD), which is a fragment of the $[M_4E_{10}]$ scaffold (AD) that is missing one ME corner, and the $[M_3E_4]$ defect-heterocubane unit (d-HC). Linking two defect-heterocubane units through two μ-bridging E atoms generates a double-defect-heterocubane $[M_6E_{10}]$ moiety (dd-HC). In the TD, d-AD, and AD units the M atoms have a tetrahedral coordination as a result of E^{2-} ligands. In the d-HC or dd-HC structures, the M atoms are usually all five coordinate in a trigonal bipyramidal arrangement. However, in some cases, one of the M···E contacts within the d-HC type unit is elongated, such that two thirds of the M atoms have a trigonal bipyramidal environment, whereas one third are situated within a tetrahedron.

SBUs of the d-HC and dd-HC type can further aggregate into structures of the general composition $\{[M_3E_7]^{2-}\}_n$,[32–35] and are discussed in Ref. [36]. These structures, which are frequently present in Sn-Se compounds, are termed here tertiary building units (TBUs). The aggregation of d-HC scaffolds through two of the three possible M atom corners yields 1D chains ($(d\text{-}HC)_C$). Aggregation of two such chains

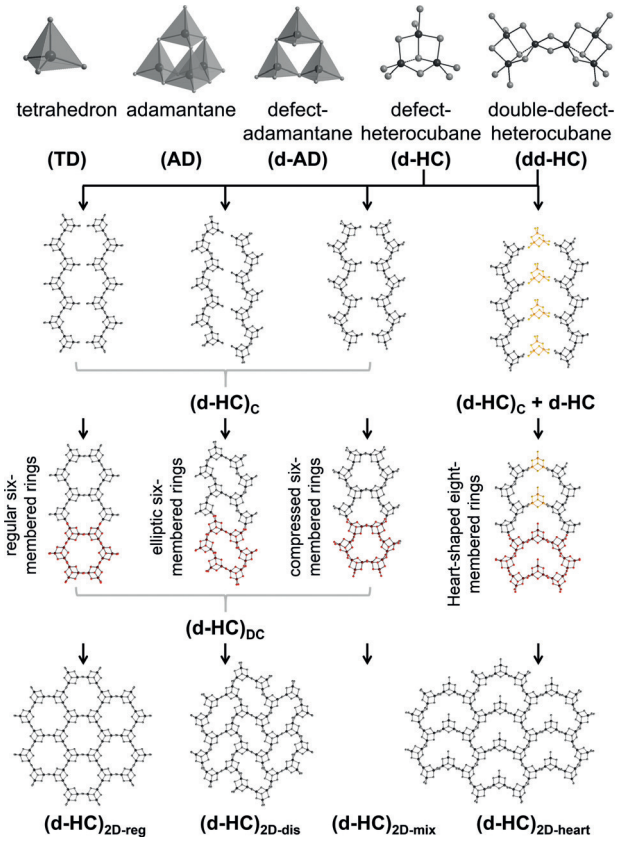

Figure 1. Secondary building units (SBUs) within chalcogenidometalate substructures (top row), which can further aggregate into tertiary building units (TBUs) with lamellar structures (2nd rows from top and bottom) and further into diverse layered structures (bottom row).

into double-chain structures ($(d\text{-}HC)_{DC}$) results in two thirds of the d-HC units being extended at all three corners. Depending on the degree of distortion within the chains, one observes more or less regular six-membered rings within the double chains. Further aggregation of those chains yields 2D layered structures with regular ($(d\text{-}HC)_{2D\text{-}reg}$) or distorted ($(d\text{-}HC)_{2D\text{-}dis}$) six-membered rings, with all the M atoms as connecting corners. Another structural motif observed for the first time in 2015 is based on heart-shaped eight-membered rings. These can be viewed as built from two $(d\text{-}HC)_C$ chains that are connected by 1/4 equivalents of further d-HC units. Further bridging by another 5/8 equivalents of other d-HC units (or by 2/3 equivalents of d-HC units starting out from the original $(d\text{-}HC)_C$ structures) produces a layered structure comprising the heart-shaped rings ($(d\text{-}HC)_{2D\text{-}heart}$). A mixed structure with alternating heart-shaped and compressed six-membered rings ($(d\text{-}HC)_{2D\text{-}mix}$) is formally obtained by combining the respective double-chain motifs. However, it is difficult to correlate the observed structural motifs with the specific reaction conditions.

3.1.2. *Molecular Compounds*

This section summarizes all the crystalline chalcogenides with molecular anions that were obtained from ionic liquids so far, either from binary or ternary solids, from the elements or from salts of chalcogenidotetrelate anions—in part together with metal nitrates or halides. One early result in the synthesis of chalcogenides from ionic liquids was the isolation of the mixed halide-chalcogenide cluster anion in $[C_2C_1im]_3[Re_3(\mu_3\text{-}S)(\mu\text{-}S)_3Br_9]Br$ (**1**), which was achieved by treatment of an $[C_2C_1im]Br\text{-}AlBr_3$ mixture with $Re_3S_7Cl_7$ at 70 °C for two days.[37] In contrast to conventional ionothermal syntheses, the resulting mixture was subsequently refluxed in acetonitrile, filtered, and then layered with diethyl ether. Dissolving the resulting black solid in acetonitrile and further layering with diethyl ether yielded single crystals. Halide exchange and abstraction of the S atoms resulted in a 0D cluster with a $[Re_3S_4]$ d-HC-type core, with each Re atom being further coordinated by three Br^- ligands (Figure 2).

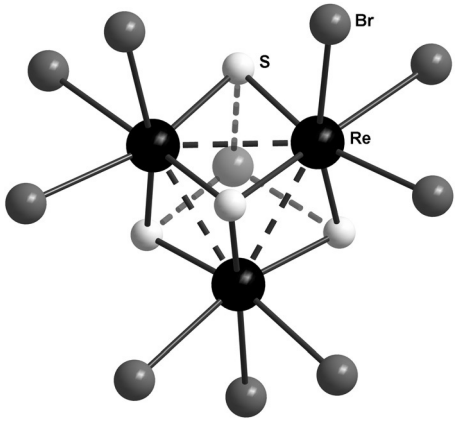

Figure 2. $[Re_3S_4]$ unit with a d-HC structure in **1** and nine bromide ligands. Weak interactions with a Br atom from an additionally cocrystallizing $[C_2C_1im]Br$ unit results in formation of a distorted HC moiety.

This cluster anion represented the first $[M_3E_4]$ (M = Mo, W, Re) cluster with nine halide ligands. Re-Re distances of 2.73–2.75 Å indicated Re-Re single bonds within an almost equilateral triangle. The d-HC core is extended to a distorted heterocubane unit (HC) through one μ_3-Br atom exhibiting longer distances to the three S atoms; this Br atom belongs to the extra $[C_2C_1im]Br$ unit that cocrystallizes within the crystal structure.

Four new nickel thiophosphates were prepared by ionothermal syntheses, starting from the corresponding elements in $[C_2C_1im][BF_4]$ at 150 °C. Single crystals of the $[C_2C_1im]^+$ salts of $[Ni(P_2S_8)_2]^{2-}$ (**2**), $[Ni(P_3S_9)(P_2S_8)]^{3-}$ (**3**), $[Ni(P_3S_9)_2]^{4-}$ (**4**), and $[(NiP_3S_8)_4(PS_4)]^{7-}$ (**5**) have been isolated along with an amorphous black powder.[38] The anionic structures of **2**–**4** contain one Ni atom each that is octahedrally coordinated by six S atoms, while in the anion of **5**, four Ni atoms are present that are octahedrally coordinated by five S and one P atom (Figure 3). In each of the compounds, P atoms are tetrahedrally coordinated by four S atoms, thereby forming different $[P_xS_y]^{n-}$ ligands. Although these were already known in the literature, their coordination modes observed in the presented structures are new. $[P_2S_8]^{2-}$ consists of two $[PS_4]$ units that share one S corner atom directly, while two other corners are bridged through another S atom to form a trisulfide group.

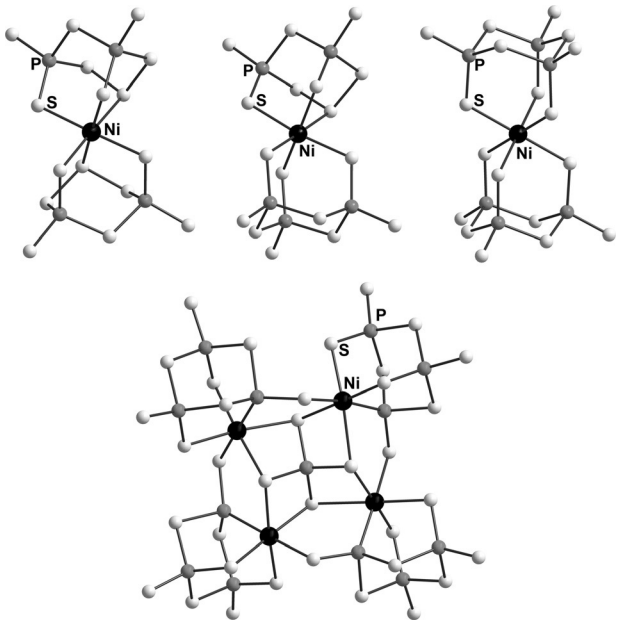

Figure 3. Molecular structures of the nickel thiophosphate anions within the salts of **2**, **3**, **4** (top, from left), and **5** (bottom).

The Ni atom in **2** is coordinated by two S atoms that bind to a P atom and the central S atom of the trisulfide group. In **3**, two different ligands coordinate the Ni atom in an octahedral manner: one $[P_2S_8]^{2-}$ ligand, which coordinates in the same manner as in **2**, and a $[P_3S_9]^{3-}$ ligand, which consists of three corner-sharing $[PS_4]$ units. Two of these $[P_3S_9]^{3-}$ ligands coordinate to a Ni atom in an octahedral fashion in **4**. A central $[PS_4]^{3-}$ unit is surrounded by four interconnected $[NiP_3S_8]^-$ groups in the relatively complex anionic structure of **5**. Each of the four Ni atoms are coordinated by two S atoms and one P atom of one $[P_3S_8]^-$ group, and one S atom of a neighboring $[P_3S_8]^-$ ligand. This is a remarkable coordination behavior of the thiophosphate ligand, which not only coordinates through the S atoms but at the same time acts as a P donor ligand.

In 2012, Huang and co-workers reported the ionothermal synthesis of a compound that comprises discrete T5-type clusters,[39] the largest clusters of the supertetrahedral T*n* family known to date, which were synthesized for the first time as isolated clusters by Feng and co-workers using organic superbases.[40] The clusters obtained by ionothermal reactions comprise ternary Cu/M/S cluster cores (M = Ga or In only) and $[C_4im]$ ligands (Figure 4). For their syntheses, mixtures of In_2S_3 and CuI, or $[enH]_2[Ga_4S_7(en)_2]$ (en = ethylenediamine) and $Cu(NO_3)_2{\cdot}3H_2O$, respectively, were treated with thioacetamide or elemental S, dimethylamine, and different amines/mineralizers (pyridine, 1,3-di(4-pyridyl)propane, 4,4′-bipyridines, or Na_2CO_3) in $[C_4C_1C_1im]Cl$ at 160 to 180 °C for five to seven days. Here, the ionic liquid not only acted as the counterion, as usually observed in ionothermal synthesis, but also as a reactive solvent that releases a $[C_4im]$ ligand. The latter coordinates to the Ga^{3+} ions at the corner of the inorganic–organic hybrid cluster anions in $[C_4C_1C_1im]_8[NH_4]_3[Cu_5Ga_{30}S_{52}(SH)_2(C_4im)_2]$ (**6**) or in $[C_4C_1C_1im]_{9.5}[NH_4]_2[Cu_5Ga_{30}S_{52}(SH)_{1.5}Cl(C_4im)_{1.5}]$ (**7**), which were obtained along with $[C_4C_1C_1im]_{12}[NH_4][Cu_5In_{30}S_{52}(SH)_2Cl_2]$ (**8**) and $[C_4C_1C_1im]_{10}[NH_4]_3[Cu_5Ga_{30}S_{52}(SH)_4]$ (**9**), which contain purely inorganic cluster anions. The $(SH)^-$, Cl^-, or $[C_4im]$ ligands at each of their corners protected the clusters from polymerization into the thermodynamically favored solids.

According to the crystal structure refinement, and confirmed by EDX and ICP-AES analyses, the clusters exhibit Cu/M ratios of 5:30. The clusters are arranged in distorted superlattices of the hexagonal (**8**, **9**) or cubic (**6**, **7**) diamond type. The cations are arranged along the faces of the tetrahedra, thus indicating that π interactions with the anions and C–H···S hydrogen bonds stabilize the clusters.

To examine the semiconducting properties of **6–9,** their optical absorption spectra were recorded (Figure 4, bottom left). These indicated band gaps of 3.68 eV (**6**), 3.62 eV (**7**), 2.28 eV (**8**), and 3.04 eV (**9**). In addition, **6**, **7**, and **9** show broad photoluminescent emission bands between $\lambda = 500$ and 800 nm, with a full-width-half-maximum (fwhm) of $\Delta\lambda =$ 180 nm when excited at $\lambda = 250$–450 nm. **8** shows a sharper emission band at $\lambda = 540$ nm with a fwhm of $\delta\lambda = 50$ nm (Figure 4, bottom right), thus similar to the Cu-In-S T5 cluster networks reported earlier.[41]

Ionothermal treatment of either chalcogenidotetrelate salts or the according element mixtures led to the formation of novel salts of rather simple or rather complex chalcogenidotetrelate anions, depending on the reaction conditions.

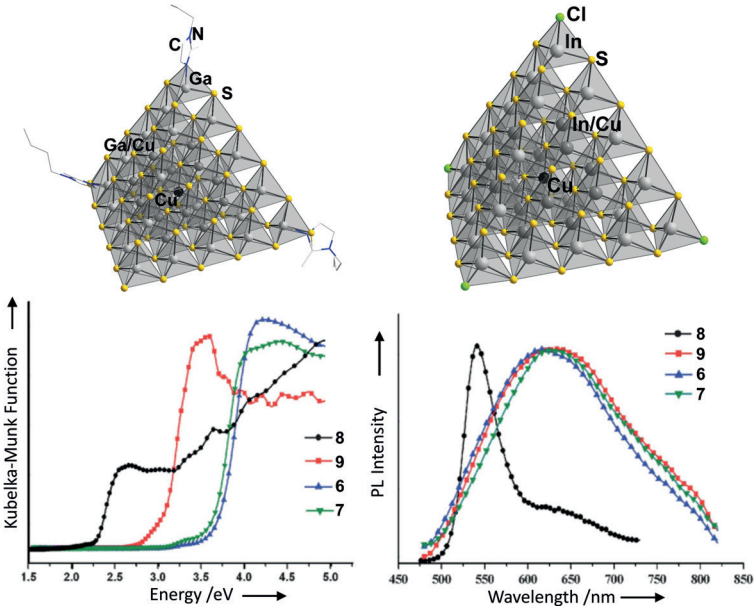

Figure 4. T5-type supertetrahedral clusters. Top left: inorganic–organic hybrid compounds shown by the example of the cluster in compound **6**. Top right: the purely inorganic cluster anion in compound **8**. Bottom left: solid-state optical absorption spectra of **6–9**. Bottom right: solid-state photoluminscence spectra of **6–9** (room temperature, $\lambda_{ex} = 370$ nm). Reproduced from Ref. [39] with permission from the Royal Society of Chemistry.

Orange plates of $[enH]_4[Sn_2Se_6]$ (**10**) were obtained upon heating $Li_4[Sn_2Se_6]$ with en in $[C_4C_1im][BF_4]$ at 100 °C for four days.[42] Interestingly, protonated en molecules and not an ionic liquid cation replaced the alkali metal cation of the starting material. The anion, which consists of two edge-sharing $[SnSe_4]$ TD units, remained unchanged.

The same simple selenidostannate anion was also formed by the ionothermal reaction of $CrCl_3{\cdot}6H_2O$, Sn, and Se in the presence of tetraethylenepentamine (tepa) or pentaethylenehexamine (peha) in $[C_2C_1im]Cl$ at 160 °C for six days.[43] The products, $[Cr(tepa)(OH)]_2[Sn_2Se_6]{\cdot}H_2O$ (**11**) and $[Cr(peha)]_2(Sn_2Se_6)Cl_2$ (**12**), are the first chalcogenidostannate salts with counterions in the form of transition-metal complexes that were synthesized by ionothermal methods. They only form under ionothermal conditions, but not in pure peha or tepa under solvothermal conditions, which produces black amorphous powders only. In **11** and **12**, the complex counterions are not bonded to the anions through metal–chalcogen bonds, such as observed for other chalcogenidostannates containing transition-metal complexes. Instead, cations and anions interact through N–H···Se, O–H···Se, and N–H···Cl hydrogen bonds, and (in **11**) through H_2O molecules, thereby producing 3D hydrogen-bonding networks.

The largest discrete polyanion consisting exclusively of main group element atoms was synthesized in 2012.[44] The so-called "zeoball" anion $[Sn_{36-x}Ge_{24+x}Se_{132}]^{24-}$ (**13**: $x = 0$; **14**: $x = 3.5$), combines a zeolite-related composition with a spherical shape and large spherical cavity (Figure 5, top left). Its outer diameter is 28.3 Å and the diameter of the inner cavity is 11.6 Å. The corresponding salts with 24 ionic liquid cations per formula unit were obtained as red crystalline blocks (Figure 5, top right) upon reaction of $[K_4(H_2O)_3][Ge_4Se_{10}]$ with $SnCl_4{\cdot}5H_2O$ in $[C_4C_1C_1im][BF_4]$ (for **13**) or $[C_4C_1im][BF_4]$ (for **14**) in the presence of a small amount of 1,3-dimethylmorpholine (DMMP) at 150 °C for two days. Remarkably, employment of the same reactants, but doubling the amount of DMMP leads to the generation of another, extended anionic structure. This indicates the subtle, but crucial influence of the auxiliary amine.

The ionic liquid cations $[C_4C_1C_1Im]^+$ or $[C_4C_1im]^+$ act as counterions that surround the anions and partially penetrate them (Figure 5, center left), thereby separating the anions that are arranged in distorted versions of the face-centered cubic lattice. The anion itself is constructed out of two SBUs, a $[Ge_3Se_9]$ d-AD and an $[Sn_6Se_{10}]$ dd-HC scaffold, which are interconnected through μ-Se bridges. The barycenters of the Ge_3 and Sn_3 triangles within the named scaffolds form a pentagon dodecahedron, such as known from the C_{20} fullerene structure.

The large windows and the large cavity inside the clusters were tested in terms of their molecular trapping and activation capability. For this, a solution of I_2 in cyclohexane was treated with the solid material. Thermogravimetric measurements indicate that the compound can reversibly take up a maximum of 11 equivalents of I_2 (Figure 5, center right). The I–I bond is then heterolytically cleaved to form I_3^- from I^- and excess I_2 (Figure 5, bottom).

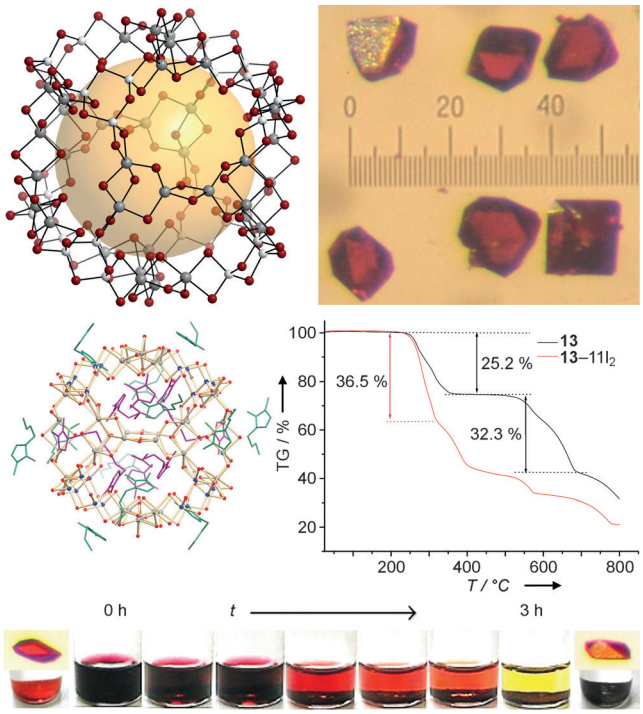

Figure 5. Top left: The so-called "zeoball" anion in **13** (shown) and **14**, with a spherical shape and a large cavity, demonstrated (yellow). Top right: photograph of crystals of **13**; each division on the scale is 0.1 mm. Center left: arrangement of counterions around the zeoball anion in the crystal structure of **13**. Center right: TGA diagram of **13** as prepared (black line) and after treatment with I_2 (red line). Bottom: fading of a solution of I_2 in cyclohexane through bond cleavage of I_2 and formation of I_3^- upon contact with solid **13**. Reproduced from Ref. [44] with permission from the American Chemical Society.

3.1.3. *Extended Structures*

Several selenidostannates with extended structures, ranging from 1D chainlike structures over 2D layered structures to 3D frameworks, have been synthesized in ionic liquids by following one of two different synthetic strategies: a bottom-up approach, starting out from the elements or precursors with small molecular precursor units, or a top-down approach, starting out from solids with 3D chalcogenide networks.

3.1.3.1. *Bottom-Up Synthesis from the Elements*

Huang and co-workers carried out comprehensive and systematic studies on reactions of Sn and Se in a 1:2.5 ratio in $[C_mC_nC_oim]Cl$. One series was run in the presence of hydrazine hydrate at 165 °C for five days.[31c] The study indicated that a small amount of hydrazine hydrate was necessary for crystallization, since in its absence, nanoparticles were formed instead of single crystals. The relative amounts of $N_2H_4{\cdot}H_2O$ (HH) and ionic liquid (IL) influences the basicity of the mixture, the phase selectivity, and thus the crystallization process as well as the crystal yields.[45] By varying this ratio (besides the chain lengths *m*, *n*, *o* of the imidazolium cation), diverse compounds were isolated with the following dimensionalities of the anionic substructure: 3D

in $[C_4C_1im]_4[Sn_9Se_{20}]$ (**15**; $m/n/o = 4:0:1$; $n_{HH}/n_{IL} = 8:5.7$), 3D in $[C_4C_1C_1im]_4[Sn_9Se_{19}(Se_2)_{0.9}Se_{0.1}]$ (**16**; $n_{HH}/n_{IL} = 1.6:5.3$), and $[C_5C_1C_1im]_4[Sn_9Se_{19}(Se_2)_{0.93}Se_{0.07}]$ (**17**) besides 2D layers in $[C_5C_1C_1im]_8[Sn_{17}Se_{38}]$ (**18**; $n_{HH}/n_{IL} = 1:4.9$) or only **18** ($n_{HH}/n_{IL} = 1.6:4.9$). A further increase in the n_{HH}/n_{IL} ratio yielded **15** for $m/n/o = 4:0:1$, or a salt with the known 2D-$[Sn_3Se_7]^{2-}$ anion with a $(d\text{-}HC)_{2D\text{-}reg}$ structure for m:1:1. All the selenidostannate substructures exhibit large pores, as indicated by the accessible volume of the crystal lattice being 55–65%, which accommodates the ionic liquid cations. The structure of **15** is the same as for **29**, which was obtained starting from $[SnSe_4]^{4-}$ just a few months earlier (see Section 3.1.3.2). The 3D anionic structures of **16** and **17** contain congruent layers perpendicular to the crystallographic *b* axis, which can be described as chains of rings of two d-HC units and four six-membered rings. Those chains are interconnected through two μ-Se atoms of every second d-HC moiety (Figure 6, top left). The other d-HC units connect to the next layer through two further μ-Se bridges (Figure 6, top right). **18** consists of several SBUs: two dd-HC assemblies are linked to an $[SnSe_4]$ TD unit by corner sharing; one Sn atom of a dd-HC unit is connected to two TD moieties such that a six-membered ring is formed; the two TD units in turn are each further connected to a d-HC scaffold; one d-HC unit is linked through two TD anions to two dd-HC assemblies and through μ-Se bridges to a six-membered ring. The SBUs are connected in such a way that several channels are formed that extend in different directions. A selection of them are shown as examples in Figure 6, along with the resulting network topology.

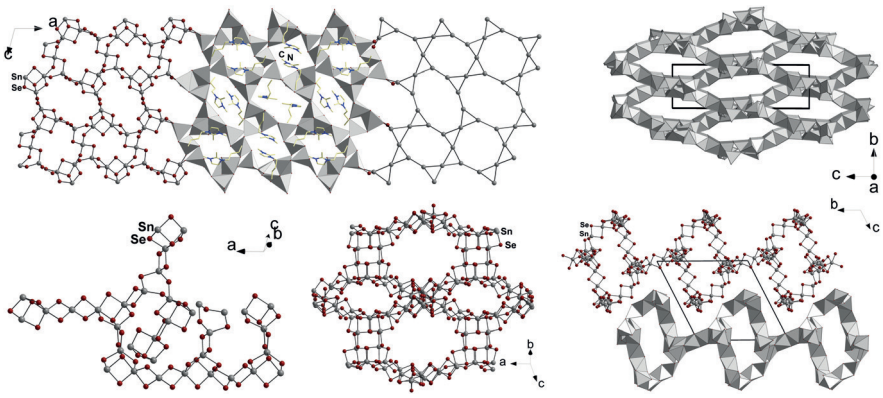

Figure 6. Top left: View onto one of the layers that are stacked perpendicular to the crystallographic *b*-axis in **16** and interconnected into a 3D anionic framework (as representative for **16** and **17**, which differ only by the nature of the cations). In addition to the ball-and-stick representation, a polyhedral view with the cations within the channels and further simplification of the network to illustrate the topology are given. Top right: polyhedral view of **16** illustrating the channels along the crystallographic *a*-axis. Bottom left: fragment of the crystal structure of **18**, which contains different structural motifs: dd-HC units, TD units, and six-membered rings. Bottom center: channels through the layers in the anionic substructure of **18**. Bottom right: channels in **18** running along the crystallographic *a*-axis within the 2D layers.

Replacing $N_2H_4{\cdot}H_2O$ by other amines, such as ethylenediamine (en) or methylamine (ma), in $[C_mC_1C_1im]Cl$ ($m = 3, 4$) yielded several 1D and 2D selenidostannate frameworks in their respective compounds through variation of the ionic liquid and auxiliary amine combination, as well as the reaction temperature and time.[33] The $[C_3C_1C_1im]^+$ salt of 2D-$[Sn_9Se_{20}]^{4-}$ (**19**; Figure 7, top) was synthesized by the reaction of Sn and Se in $[C_3C_1C_1im]Cl$ in the presence of ma ($n_{ma}/n_{IL} = 5.7:1.8$) at 160 °C for five days. Replacing ma by en, and decreasing the reaction temperature to 140 °C ($n_{en}/n_{IL} = 5.0:1.4$) yielded 1D-$[Sn_3Se_7]^{2-}$ in $[C_3C_1C_1im]_2[Sn_3Se_7]$ (**20**). Prolonging the reaction time led to the formation of $[C_3C_1C_1im]_2[Sn_3Se_7]$ (**21**), with 2D-$[Sn_3Se_7]^{2-}$ anions, besides **20**, while **21** was isolated as a pure phase upon increasing the reaction temperature to 160 °C ($n_{en}/n_{IL} = 5.7:2.9$). 1D-$[Sn_3Se_7]^{2-}$ anions in $[C_4C_1C_1im]_2[Sn_3Se_7]$ (**22**) were obtained when carrying out the reaction in $[C_4C_1C_1im]Cl$ in the presence of en at 140 °C for five days ($n_{en}/n_{IL} = 5.3:1.4$). The compound was formed in addition to $[C_4C_1C_1im]_2[Sn_3Se_7]$ (**23**) with a 2D-$[Sn_3Se_7]^{2-}$ anion upon extending the reaction time to 15 days. Pure **23** was obtained by treatment at higher temperature (160 °C). Although possessing the same nominal composition, the anions within **20**–**23** vary in their structural details. **19** contains 2D layers that are based on two SBUs, the $[Sn_6Se_{10}]$ dd-HC unit and an $[Sn_3Se_{10}]$ unit consisting of three corner-sharing TD moieties. Rings consisting of two of each of the SBUs extend into layers, which are separated from each other by the cations of the ionic liquid. The structure of the anion in **20** is similar to the well-known $(d\text{-}HC)_C$ chain motif. The anionic substructure of **22** consists of double chains of $(d\text{-}HC)_{DC}$, and further aggregation to the regular honeycomb-like structure $(d\text{-}HC)_{2D\text{-}reg}$ is observed for **21** and **23**.

Further structural diversity can be achieved by adding another metal component to the mixtures—for example, a transition-metal chloride, which was realized with AgCl or $MnCl_2{\cdot}4H_2O$. The addition of AgCl to a reaction mixture containing Sn and Se in $[C_4C_1C_1]Cl$ in the presence of $N_2H_4{\cdot}H_2O$ ($n_{HH}/n_{IL} = 5.3:4.5$) and heating to 160 °C for five days yielded $[C_4C_1C_1im]_7[AgSn_{12}Se_{28}]$ (**24**) with $[AgSn_{12}Se_{28}]^{7-}$ anions, which is a rare example of heterometallic chalcogenides being obtained from ionothermal reactions.[33] Within the anion, $(d\text{-}HC)_{DC}$ moieties are linked by linearly coordinated silver ions (Figure 7, 2nd from top). A different observation was made upon addition of $MnCl_2{\cdot}4H_2O$ in the presence of chelating amines, such as en or diethylenetriamine (dien): metal–amine complexes are formed, which compete with the ionic liquid cations for the role of the structure-directing agent and the counterion.[36] One equivalent of Sn and 2.5 equivalents of Se were combined with $MnCl_2{\cdot}4H_2O$ in the presence of amine in three equivalents of $[C_4C_1C_1im]Cl$ at 160 °C for five days. $[Mn(en)_3][Sn_3Se_7]$ (**25**) was obtained by using eight equivalents of en. Replacement of en by five equivalents of dien yielded $[Mn(dien)_2][Sn_3Se_7]{\cdot}H_2O$ (**26**).

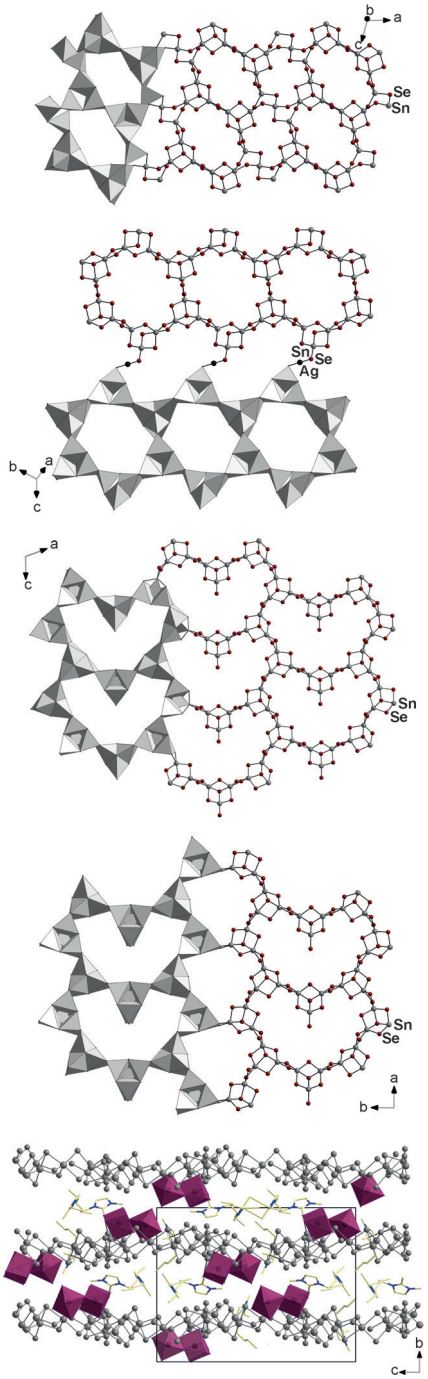

Figure 7. View of one of the anionic layers in **19**, **24**, **27**, and **28** (from top), which contain different ring structures. Bottom: packing of anions (gray spheres) and cations in **27**. The Mn complex cations are shown as purple octahedra and the ionic liquid cations are drawn as yellow-blue wires.

Increasing the amount of $[C_4C_1C_1im]Cl$ to five equivalents led to the formation of $[C_4C_1C_1im]_3[Mn(en)_3]_2[Sn_9Se_{21}]Cl$ (**27**) in the presence of en, or to $[C_4C_1C_1im]_6[Mn(dien)_2]_2[Sn_{15}Se_{35}]$ (**28**) in the presence of dien.

All the compounds possess lamellar 2D-$[Sn_3Se_7]^{2-}$ anions, with different sized rings. All of them consist of $[Sn_3Se_4]$ d-HC units that are bridged by two μ-Se atoms and differ in structural details, depending on the nature of the counterions that separate and connect the anionic layers: ammonium cations, such as the ionic liquid cations, lead to the formation of regular layers of the $(d\text{-}HC)_{2D\text{-}reg}$ type. Metal–amine complexes such as $[Mn(en)_3]^{2+}$ or $[Mn(dien)_2]^{2+}$ lead to the layers containing distorted hexagonal rings, $(d\text{-}HC)_{2D\text{-}dis}$, as in **25** and **26**. In **27**, the network is based on novel eight-membered, heart-shaped rings that are further assembled into a 2D structure ($(d\text{-}HC)_{2D\text{-}heart}$, Figure 7, center and bottom). In **28**, those rings alternate with a third variant of the six-membered rings, with the two bridging μ-Se atoms being folded to the inside of the rings rather than to the outside in three of the six bridging positions ($(d\text{-}HC)_{2D\text{-}mix}$; Figure 7, 2nd from bottom).

The competitive and synergistic effects of metal–amine complexes and imidazolium cations on the structures were investigated in detail in this study. A large excess of ionic liquid with respect to the amount of the metal complex, beyond 6:1, did not yield crystalline products. Decreasing this ratio to 5:1 or 4:1 resulted in both the ionic liquid cation and the complex cation acting as structure-directing agents, thereby leading to the formation of the heart-shaped rings within the anionic substructures. Further decreasing the ratio to 3:1 yielded compounds exclusively featuring metal–amine complexes as cations that stabilize the $(d\text{-}HC)_{2D\text{-}dis}$ anion structure. Although it is still not possible to explain the formation of the diverse structures under the different conditions, nor to predict any of the products a priori, the observations clearly indicate the importance in the choice of the reaction conditions and reactants, as the ionic liquid cation as well as the amines or the metal amine complexes potentially interact with the anions or parts of them or with each other through hydrogen bonding or anion–π interactions.

3.1.3.2. ***Bottom-Up from Binary or Ternary Molecular Anions***

Extended chalcogenide structures can also be accessed from small binary or ternary molecular anions, such as indicated above for molecular anions, and as reported for reactions in protic solvents.[4b,17] Treatment of $[K_4(H_2O)_4][SnSe_4]$ in $[C_4C_1im][BF_4]$ for seven days over a wide temperature range (130–180 °C) provided a compound with a 3D-$[Sn_9Se_{20}]^{4-}$ substructure (**29**) in different yields.[46] This 3D framework comprises $[Sn_6Se_{10}]$ dd-HC units with all the Sn atoms being surrounded by five Se atoms in a trigonal bipyramidal manner. Each of the resulting "terminal" Se atoms are connected to an $[SnSe_4]$ TD moiety through edge bridging. Four of the resulting $[Sn_7Se_{14}]$ zigzag chains are finally interconnected by $[Sn_2Se_6]$ spacers to form a 3D framework (Figure 8, top and second from top). The structure possesses an accessible volume of 56.8 %, which accommodates the $[C_4C_1im]^+$ cations.

This strategy was extended by using $[K_4(H_2O)_3][Ge_4Se_{10}]$ along with $SnCl_4{\cdot}5H_2O$ as a second metal component.[47] In the presence of a small amount of DMMP in $[C_4(C_1)C_1im][BF_4]$, this yielded the above-described zeoball anion in **13** and **14**. Further variations of the reaction conditions, in terms of the Sn/Ge ratio as well as the nature and amount of amine

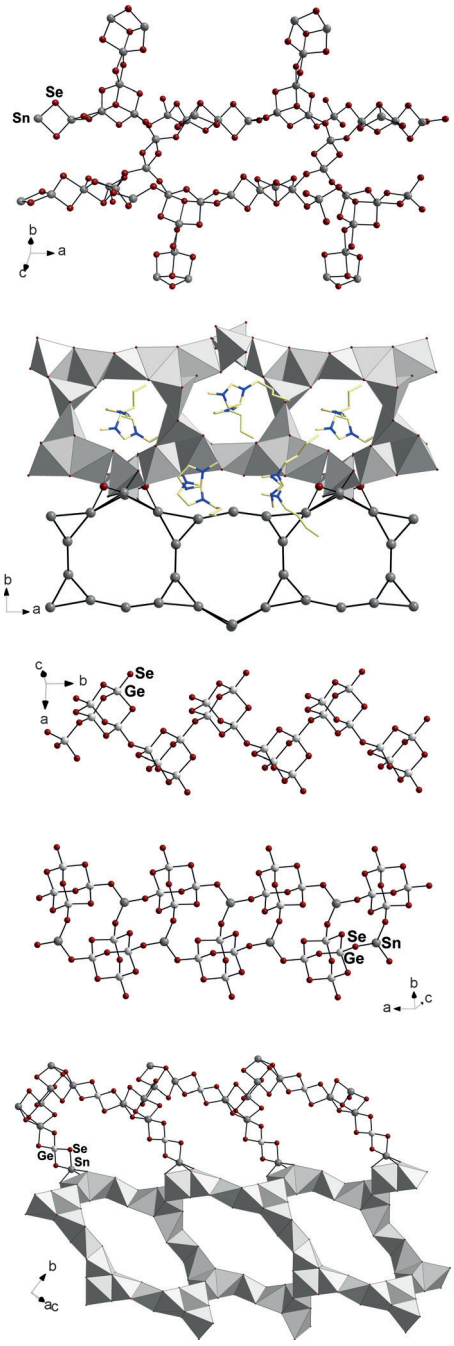

Figure 8. Binary or ternary anionic substructures with different network topologies, obtained from binary precursor anions by ionothermal treatment of $[K_4(H_2O)_4][SnSe_4]$ or $[K_4(H_2O)_3]Ge_4Se_{10}]$ together with $SnCl_4{\cdot}5\,H_2O$, respectively. Top: 3D network in **29**. Second picture from top: Illustration of the channels along the crystallographic *c*-axis and the network topology in compound **29**. Center: Fragment of the 1D chains in **30**. Second picture from bottom: Fragment of a 1D chain in **31**. Bottom: Fragment of a 2D layer in **32**.

(DMMP versus en) as the most subtle parameter, or by using $SnCl_2$ instead of $SnCl_4{\cdot}5\,H_2O$, yielded compounds with several different anion topologies. These varied from binary 1D-$[Ge_4Se_9]^{2-}$ chains in $[C_4C_1im]_2[Ge_4Se_9]$ (**30**) or ternary 1D-$[Ge_4SnSe_{10}]^{2-}$ anions in $[C_4C_1C_1im][SnGe_4Se_{10}]$ (**31**) through ternary 2D-$[Sn_{3.17}Ge_{0.83}Se_{8.94}(Se_2)_{0.06}]^{2-}$ layers in $[C_4C_1C_1im]_2[Sn_{3.17}Ge_{0.83}Se_{8.94}(Se_2)_{0.06}]$ (**32**) to binary 3D-$[Sn_9Se_{20}]^{4-}$ networks in $[C_4C_1im]_4[Sn_9Se_{20}]$ (**29**) or 3D-$[Sn_{18}Se_{40}]^{8-}$ networks in $[C_4C_1C_1im]_8[Sn_{18}Se_{40}]$ (**33**). **30** could only be synthesized along with the zeoball compound when the Sn/Ge ratio within the reactant mixture was lowered from 2:3 (the ratio to synthesize the zeoball anion) to 2.3:5; **30** contains no Sn atoms and the anionic substructure represents zigzag chains of corner-linked $[Ge_4Se_{10}]$ AD units (Figure 8, center). The use of $SnCl_2$ instead of $SnCl_4$ and increasing the reactant Sn/Ge ratio to 4.6:5 led to the formation of **31**. The anion is composed of double chains of $[Ge_4Se_{10}]$ AD units that are linked through Sn^{2+} ions (Figure 8, 2nd from bottom). The formal oxidation state of the Sn atom is clearly reflected in a pyramidal coordination mode, with one structurally active lone pair of electrons. Hence, the choice of this reactant served to direct the structure assembly away from the formation of the known 3D-$[MGe_4Se_{10}]^{2-}$ network, which tends to result from reactions of $[T_4E_{10}]^{4-}$ anions with M^{2+} cations if the latter do not possess a lone pair of electrons (for example, with T = Ge, Sn; E = S, Se; M = Mn, Fe, Cu_2, Ag_2, Ag).[48] **32** can be obtained in pure form by using en exclusively as the auxiliary in the reaction mixture. The anionic structure consists of 2D-$[GeSn_3Se_9]^{2-}$ layers that are constructed through linkage of $[Sn_6Se_{10}]$ dd-HC and $[GeSe_4]$ TD units through μ-Se bridges into large rings (Figure 8, bottom). If a dd-HC scaffold is considered as two d-HC units, these rings are eight-membered and consist of a total of 32 atoms.

32 was the first compound to contain this kind of anionic structure with a ternary composition. The use of a larger amount of en in $[C_4C_1im][BF_4]$ under otherwise unchanged conditions allowed an alternative access to **29**, which can also be approached starting from the elements or from $[K_4(H_2O)_4][SnSe_4]$ (see above). Compound **33** was synthesized in the same way as **29**, but using the ionic liquid $[C_4C_1C_1im][BF_4]$. Neither **29** nor **33** contain any Ge atoms, although the second route to **29** involved a source for them. The main building unit of the anionic structures of both compounds is the dd-HC structure, which is further connected into different 3D networks.

Recently, further variations in the added amine have been examined by using the original reactant ratio for the formation of **13**, but at lower temperature (120 °C) and extension of the reaction time. Replacement of DMMP with diazabicyclo[2.2.2]octane (DABCO) led to the formation of **13**, aminoethylpiperazine (aep) produced a compound with a $(d\text{-}HC)_{2D\text{-}reg}$ network, while using 4,4′-trimethylenedipiperidine (tmdp) yielded crystals of both.

The reaction behavior of ternary molecular precursors was recently explored by treatment of alkali metal salts of the P1-type cluster anion $[Mn_4Sn_4Se_{17}]^{10-}$ (P1 represents the smallest member of the supertetrahedral P*n* cluster family).[49] In this way, $[Mn(en\text{-}Me)_{0.5}en_{2.5}][Sn_3Se_7]$ (**34**), a compound composed of all three components of the reactant anion, was obtained. However, the components were not combined in an extended ternary anionic substructure, instead the compound consists of the $(d\text{-}HC)_{2D\text{-}dis}$ anion and complex cations. Remarkably, an in situ methylation of en by reaction with the ionic liquid cation takes place under

the given reaction conditions, which serves to further stabilize the structure by enhanced anion–cation interactions through the additional methyl group.

3.1.3.3. The Top-Down Approach

The 3D framework in $K_2Sn_2Se_5$[50] undergoes a stepwise, temperature-controlled deconstruction in $[C_4C_1C_1im][BF_4]$ (Figure 9).[51] Heating $K_2Sn_2Se_5$ to 120 °C for four days results in its conversion into $[C_4C_1C_1im]_{16}[Sn_{24}Se_{56}]$ (**35**), with a $(d\text{-}HC)_{2D\text{-}reg}$-type 2D-$[Sn_{24}Se_{56}]^{16-}$ anion. Further heating to

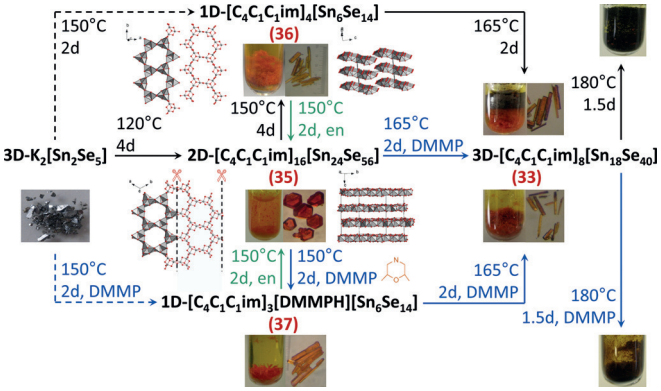

Figure 9. Temperature-controlled transformation of chalcogenidostannate substructures, starting from a 3D network in $K_2Sn_2Se_5$. Details are given in the text; d = days.

150 °C for another four days yields $[C_4C_1C_1im]_4[Sn_6Se_{14}]$ (**36**), which is based on an anionic 1D-$[Sn_6Se_{14}]^{4-}$ $(d\text{-}HC)_{DC}$ structure. The addition of DMMP at this step and heating for only two days produced the same anionic substructure, but led to the incorporation of protonated amine as counterions in $[C_4C_1C_1im]_3[DMMPH][Sn_6Se_{14}]$ (**37**). **36** and **37** differ only slightly in the packing of their $(d\text{-}HC)_{DC}$ anionic strands within the crystal and the interaction of the latter with the different counterions.

It is noteworthy that the transformation from the 2D substructure in **35** into the 1D substructures does not change the elemental composition, only the coordination numbers of one sixth of the Sn atoms. The reason for this is the splitting of a part of the dd-HC units with two doubly μ-Se-bridged d-HC moieties into separate d-HC units with terminal Se atoms. According to quantum chemical investigations, each of these Sn–Se contacts adds 50 kJ mol^{-1} to the total energy of the compounds, in line with the necessity of further heating for breaking the bond. The reverse reaction pathway—from 1D back to 2D—is possible by tempering the crystals within the ionic liquid upon addition of en at 150 °C for two days. The amine seems to trigger Sn-Se bond formation by interim hydrogen bonding. Other studies on the effect of different amines also pointed in this direction: both the basicity (alkyl/aryl amine, chain length) and the number of potential hydrogen-bridging sites (primary, secondary, tertiary amine) substantially affect the extent of the network formation.

The 1D compounds are also directly accessible by treating $K_2Sn_2Se_5$ at 150 °C for two days without amine (**36**) or with DMMP (**37**). **35**–**37** can be further converted into the aforementioned compounds **29** or **33** with $[Sn_{18}Se_{40}]^{8-}$ 3D frameworks by treatment in $[C_4C_1C_1im][BF_4]$ at 165 °C for two days with or without DMMP. At 180 °C, the crystals are finally destroyed, with formation of a black powder.

3.1.4. Optoelectronic Properties of Polyanionic Chalcogenides

Investigation of the optoelectronic properties of the compounds indicate that the ionothermal treatment allows for the generation of chalcogenides with subtly differing electronic properties as a result of their compositions and structures. The selenidometalates mentioned in Section 3.1.3, for example, are orange to red, which is in accordance with their electronic excitation energies of $E_{ee} = 1.9$–2.3 eV (Figure 10).

Although having similar porosities (accessible volumes of 57–67 %), the structures differ in terms of the dimensionality

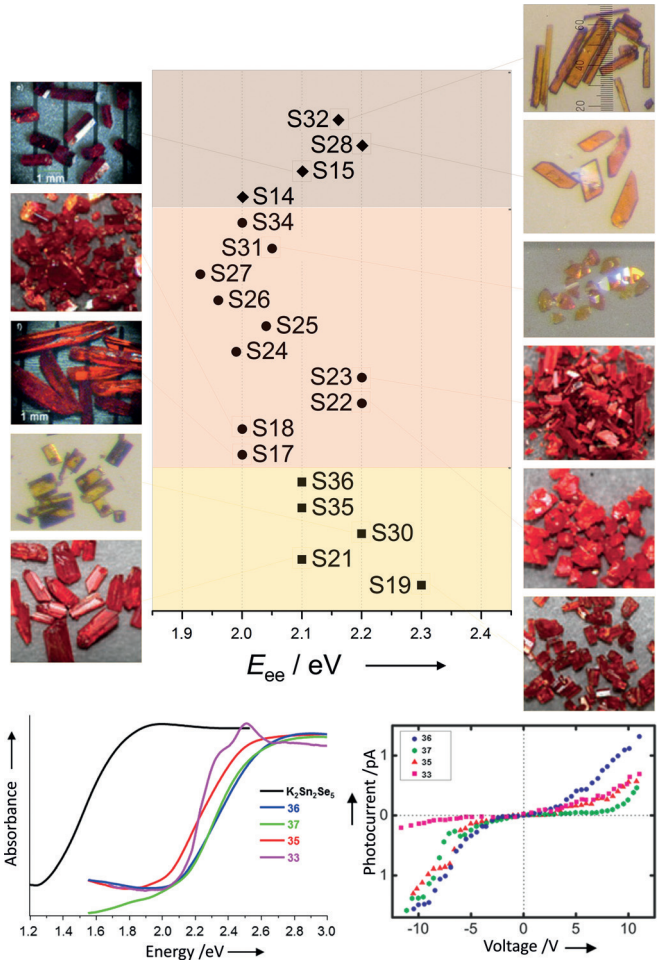

Figure 10. Optical properties of crystalline chalcogenides that were obtained from ionic liquids. Top: comparison of the E_{ee} values of selenidostannate compounds of different dimensionalities, along with photographs of the respective single-crystalline materials. Bottom: UV/Vis spectra (left) and photocurrent (right) of compounds with Sn-Se frameworks of different dimensionalities, generated by phase transformation starting from $K_2Sn_2Se_5$. Reproduced from Ref. [51] with permission from Wiley-VCH.

and elemental composition, including the presence or absence of transition-metal ions. As all of these parameters contribute subtly to the electronic excitation energies, only series of related compounds should be compared with each other, such as shown in Figure 10 (bottom).

3.2. Polycationic Chalcogenides

Polycationic chalcogenides represent an interesting subgroup of chalcogenide compounds. They can be conceptually derived from main-group homo-polycations, such as Bi_5^{3+} or Te_4^{2+}, and have been traditionally prepared in acidic, electrophilic media such as oleum or in molten $Na[AlCl_4]$. Given that the origin of ionic liquid research was the search for the replacement of such media in batteries,[52] the use of Lewis-acidic ionic liquids containing chloridotrielate anions appears to be a logical step in the extension towards new reaction conditions. The ionic liquids used are typically prepared as mixtures of $[C_nC_1im]X$ and AlX_3 or GaX_3 (X = Cl, Br), thus distinctly different from the basic reaction media that are generally used for polyanionic chalcogenides (except for compound **1**). The reactions start out from the elements, a chalcogen, and a main-group metal, with or without the addition of a metal or chalcogen chloride (aside from the ionic liquid constituent) to further adjust the redox properties of the mixture. Common variations include the addition of mixed halide systems, oxidizers such as $NbCl_5$, or auxiliaries such as NaCl. Reaction and crystallization at room temperature is possible within a few days, but reaction temperatures of up to 200 °C are also reported. Yields are often good, 50 % and higher. The formation of chalcohalide compounds is frequently observed, with bromide anions serving as ligands to the metal atoms in the cationic cluster compounds. Chloridotrielate complexes serve as weakly coordinating counterions, usually as $[MCl_4]^-$ anions (M = Al, Ga), with some rare examples of higher degrees of aggregation. The incorporation of chloridotrielate ions tends to make most compounds moisture sensitive.

The use of ionic liquid reaction media has allowed researchers to extend the century-old and well-documented chemistry of main-group homo-polycations, and the somewhat newer results on hetero-polycations, towards previously unknown compounds. These can be understood with the Zintl–Klemm pseudo-element concept in some cases, but often display quite complicated electronic situations. This includes metal–metal bonding, "formal" chalcogenide anions that, however, carry a (partial) positive charge upon closer inspection by quantum chemical methods, charge delocalization, or multicenter bonding.[53] In contrast to the polyanionic chalcogenides discussed above, most of the observed structures are based on heterocubane-type SBUs (HC).

The first example of a polycationic chalcogenide compound synthesized in an ionic liquid was presented by Kanatzidis and co-workers in 2009.[31a] $[Sb_7S_8Br_2](AlCl_4)_3$ (**38**) was obtained as red crystals upon reacting Sb and S in a mixture of $[C_2C_1im]Br$ and $AlCl_3$ at 165 °C for ten days. In the $[Sb_7S_8Br_2]^{3+}$ cation, two $[Sb_2S_2]$ HC units share a common corner. Additionally, two bromide ions serve as ligands to two Sb ions. A fragment of the crystal structure is shown in Figure 11 (top). **38** has an optical band gap of 2.03 eV (Figure 11, center row left) and displays nonlinear optical properties as a result of its non-centrosymmetric structure. It can be used for second harmonic generation and difference frequency generation (Figure 11, center row right and bottom).

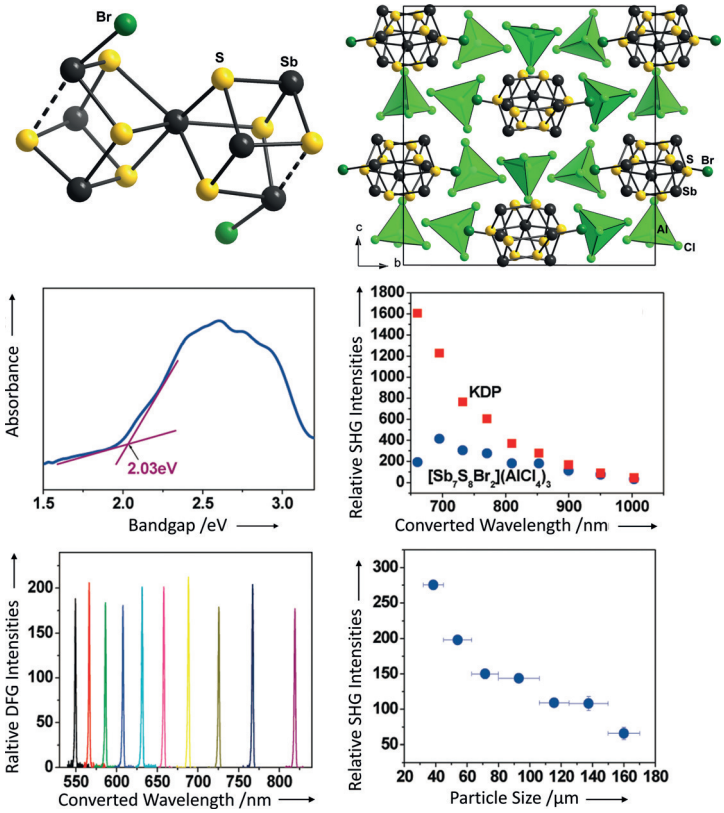

Figure 11. Top left: $[Sb_7S_8Br_2]^{3+}$ cation in **38**, with secondary interactions marked as dashed lines. Top right: Packing of polycations and $[AlCl_4]^-$ counterions in the crystal structure of **38**. Center left: electronic absorption spectrum of a single crystal of **38**. Center right: second harmonic generation (SHG) of **38** (blue) relative to the benchmark SHG material KH_2PO_4 (red). Bottom left: difference-frequency generation (DFG) with polycrystalline **38**. Bottom right: particle-size dependence of the SHG intensity generated from polycrystalline **38**. Reproduced from Ref. [31a] with permission from the American Chemical Society.

Ruck and co-workers have presented another molecular polycation in $[Sb_{10}Se_{10}][AlCl_4]_2$ (**39**), which was synthesized from Sb, Se, and $SeCl_4$ in a mixture of $[C_4C_1im]Cl$ and $AlCl_3$ at room temperature.[54] Black crystals of the compound were obtained after four days. The $[Sb_{10}Se_{10}]^{2+}$ cation in **39** is composed of two realgar-like $[Sb_4Se_4]$ cages, interconnected by a planar $[Sb_2Se_2]$ ring (Figure 12, top left). The connectivities of the atoms can be rationalized with the Zintl–Klemm concept, but a complicated Raman spectrum (Figure 12, top right) as well as quantum chemical investigations (Figure 12,

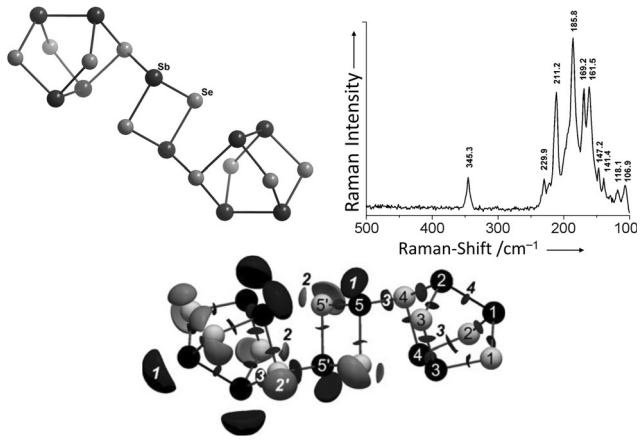

Figure 12. Top left: $[Sb_{10}Se_{10}]^{2+}$ cation in **39**. Top right: Raman spectrum of a single crystal of **39** showing the symmetric stretching mode of the $[AlCl_4]^-$ anion at $\tilde{\nu}=345\ cm^{-1}$ and bands belonging to the polycation between $\tilde{\nu}=230$ and $100\ cm^{-1}$. Bottom: localization domains 1–4 calculated for the $[Sb_{10}Se_{10}]^{2+}$ polycation using the electron localizability indicator (ELI-D; Y_D^{σ}).[56] Sb: black, Se: light gray. 1: lone pair of electrons on the Sb atoms (not depicted for the right $[Sb_4Se_4]$ realgar-like cage to enhance readability; U = 1.455); 2: lone pairs of electrons on two-bonded Se atoms (U = 1.49); 2′: lone pair of electrons on three-bonded Se atoms (U = 1.455); 3: Sb–Se bond (U = 1.31–1.33); 4: Sb–Sb bond (U = 1.315). Reproduced from Ref. [54] with permission from Wiley-VCH.

bottom) show that the electronic situation is a bit more involved.

Further exploration of the Sb-Se elemental combination in more bromine rich ionic liquids by Ruck and co-workers yielded an interesting series of compounds that demonstrated the crucial influence of the halide ions and oxidants such as $NbCl_5$ in the reaction mixture.[55] Combining Sb, Se, and $NbCl_5$ in an ionic liquid prepared from $[C_4C_1im]Br$ and $AlBr_3$, and performing the reaction at 160 °C for seven days, affords red crystals of $[Sb_7Se_8Br_2][AlX_4]_3$ (**40**; X = Cl, Br in various proportions). **40** is the isostructural selenium analogue of **38**. The same procedure, but omitting $NbCl_5$ and working in a more chloride rich ionic liquid, namely a mixture of $[C_4C_1im]Br$ and $AlCl_3$, produced a different polycationic chalcohalide compound, $[Sb_{13}Se_{16}Br_2][AlCl_{3.2}Br_{0.8}]_5$ (**41**), as dark-red crystals.

The use of the bromide-rich ionic liquid $[C_4C_1im]Br/AlBr_3$ and omitting $NbCl_5$ leads to a formal double salt of **40** and **41**, namely $[Sb_{13}Se_{16}Br_2][Sb_7Se_8Br_2][AlBr_4]_8$ (**42**), as red crystals. $[Sb_{13}Se_{16}Br_2]^{5+}$ represents the largest known molecular main group metal polycation. It is similar to $[Sb_7Se_8Br_2]^{3+}$, but composed of four instead of just two corner-sharing HC units, again with bromide ligands terminating the outermost antimony atoms (Figure 13, top left; packing of cations and anions: top right).

In another extension of their studies of the Sb-Se system, Ruck and co-workers presented $[Sb_2Se_2]AlCl_4$ (**43**), a compound containing the one-dimensional polycation 1D-$[Sb_2Se_2]^+$.[57] Dark-red crystals of **43** were prepared from Sb and Se in an ionic liquid composed of $[C_4C_1im]Cl$ and $AlCl_3$, by heating to 160 °C for one week. Thermogravimetric measurements showed that **43** starts forming at 160 °C and decomposes at 190 °C. This underlines that the reaction temperature can be a key parameter in the formation of different polycationic chalcogenides. The 1D-$[Sb_2Se_2]^+$ polycationic chain in **43** is composed of three different types of $[Sb_2Se_2]$ rings that form a pair of face-sharing HC scaffolds interconnected through a distinctly shifted and rotated ring (Figure 13, bottom center; packing of cations and anions: center left). A wide range of Sb-Se distances is observed, thus complicating the analysis of the electronic situation in the cation (Figure 13, bottom left). Quantum chemical investigations indicated that the Zintl–Klemm concept cannot be applied in this case (Figure 13, bottom right).

Kanatzidis and co-workers reported an isostructural class of layered, polycationic chalcohalide compounds, 2D-$[Bi_2Te_2Br](AlCl_4)$ (**44a**), 2D-$[Sb_2Te_2Br](AlCl_4)$ (**44b**),[31b] and 2D-$[Bi_2Se_2Br](AlCl_4)$ (**44c**).[58] Black crystals of all three compounds were synthesized from the elements in a mixture of $[C_2C_1im]Br$ and $AlCl_3$ within seven days at 165 °C. The layered 2D-$[Bi_2Te_2Br]^+$ cation is composed of ribbons of $[Bi_2Te_2]$ rings connected into layers through Br atoms, as shown in Figure 14 (top). **44a** is a strongly anisotropic direct band gap semiconductor, as shown by measurements of the optical and electrical properties, as well as calculations of the electronic band structure and density of states (Figure 14, bottom).

By using the same reaction system and parameters as for **44a**, but changing the Bi/Te ratio from 1:1 to 1:3, Kanatzidis and co-workers have also obtained black crystals of the polycationic framework compound $[Bi_4Te_4Br_2(Al_2Cl_{6-x}Br_x)](AlCl_4)$ (**45**), a compound structurally very similar to **44a** apart from a variation in the Cl/Br ratio.[58] Measurements of the optical and transport properties, as well as calculations of the band structure show that **45** is an n-type semiconductor with a narrow, indirect band gap.

In addition to the pseudo-binary polycationic chalcogenides, two other examples exist of compounds containing multinary polycations. Freudenmann and Feldmann reacted Bi, S, and $BiCl_3$ in a mixture of $GaCl_3$ and $[C_4C_1im]Cl$ for ten days at 150 °C to obtain red crystals of $[Bi_3GaS_5]_2[Ga_3Cl_{10}][GaCl_4]\cdot S_8$ (**46**).[59] The compound is composed of several unusual components. The chloridogallate anion $[Ga_3Cl_{10}]^-$ possesses an unprecedented star-shape aggregation motif and the capture of S_8 within the highly ionic compound is also intriguing, especially considering that elemental sulfur was not used in a large excess in the reaction mixture. The $[Bi_3GaS_5]^+$ cation displays a distorted HC motif (Figure 15, top left), which is in accordance with the Zintl–Klemm concept.

Ruck and co-workers described the synthesis of a series of multinary, polycationic compounds with the composition $M_2Bi_2S_3(AlCl_4)_2$ (M = Ag, Cu; **47**), and found two polytypes for M = Cu.[60] The synthesis of the compounds can be performed under various conditions, with or without an ionic liquid, from different binary or multinary starting materials. The 2D-$[M_2Bi_2S_3]^{2+}$ layers in all three compounds consist of trigonal bipyramidal $[Bi_2S_3]$ units, interconnected with M^+ ions into hexagonal layers (Figure 15, bottom left and right).

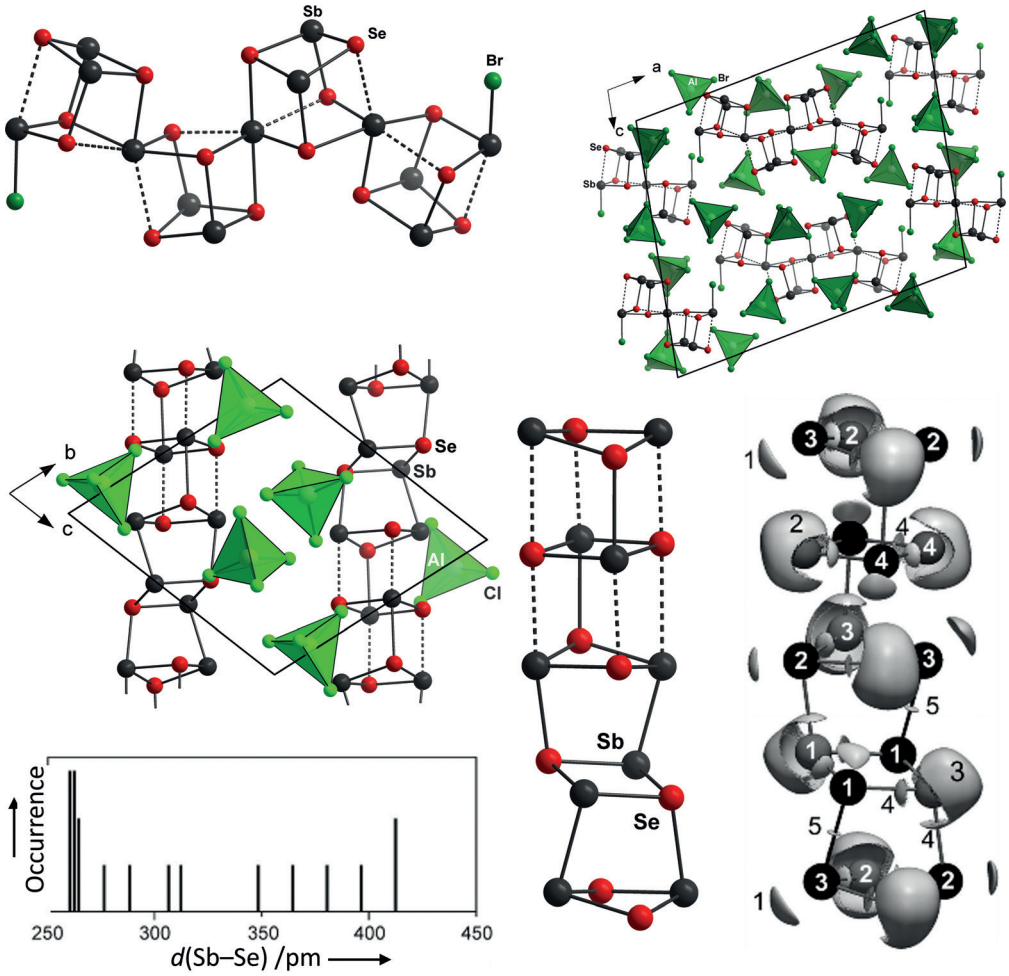

Figure 13. Top left: the $[Sb_{13}Se_{16}Br_2]^{5+}$ cation in **42**, with secondary interactions indicated by dashed lines. Top right: packing of $[Sb_{13}Se_{16}Br_2]^{3+}$ and $[Sb_7Se_8Br_2]^{5+}$ polycations along with the $[AlBr_4]^-$ counterions within the crystal structure of **42**. Center left: packing of the polycationic chain 1D-$[Sb_2Se_2]^+$ with the $[AlCl_4]^-$ counterions in the crystal structure of **43**. Bottom left: Histogram of interatomic distances Sb-Se in the crystal structure of **43**. Bottom center: Fragment of the polycationic chain in **43**, with secondary interactions indicated by dashed lines. Bottom right: ELI-D localization domains (depicted at $Y = 1.3$) for 1D-$[Sb_2Se_2]^+$ (Sb: black, Se: light gray): 1: lone pair of electrons on the Sb atoms; 2: lone pairs of electrons on two-bonded Se atoms merged into one domain; 3: lone pair of electrons on three-bonded Se atoms; 4: Sb–Se bond; 5: Sb–Sb bond.[56] Reproduced from Ref. [57] with permission from Wiley-VCH.

Another unique case was presented by Huang and co-workers. From a mixture of $CrCl_3$, S, $[C_4C_1C_1im]Cl$, urea, and hydrazine hydrate, they obtained air-stable, black crystals of $[Cr_7S_8Cl_2(NH_3)_{14.5}(H_2O)_{1.5}]Cl_3{\cdot}H_2O$ (**48**) after six days at 160 °C.[61] **48** is unusual in several ways: it was obtained from a basic reaction mixture, which usually yields chalcogenidometalate anions and not polycationic compounds (cf. the uncommon synthesis conditions for the generation of compound **1**). Additionally, it is a unique example of a chromium-based double-HC-type cluster that carries only inorganic ligands (Figure 16, top). Measurements of the magnetic properties of **48** revealed antiferromagnetic coupling of the metal ions (Figure 16, bottom).

Studies by Beck and co-workers should also be mentioned. Although the studies were mostly carried out in low-temperature melts of inorganic salts, such as aluminum or gallium halides, thereby obtaining many examples of polycationic compounds, they frequently employed auxiliaries such as tetraphenylphosphonium chloride for the in situ formation of ionic liquids.[62] This emphasizes the close relationship between the reactions in molten salts and ionic liquids—often, a combination of both approaches can help to achieve the formation of single crystals as pure phases for further analyses.

3.2.1. *Optoelectronic Properties of Polycationic Chalcogenides*

The properties of polycationic chalcogenide compounds have not so far been explored in very great detail, presumably because of their sensitive nature. However, in a few cases the optical absorption spectra of these compounds have been measured and the respective quantum chemical investigations have been performed to determine the band structure. Although there is not enough data to deduce any detailed relationships between the structure and the optical properties, general trends found in other chalcogenide materials are also well reflected here: heavier chalcogens will produce compounds with smaller band gaps, as seen for the reported E_{ee} values of compounds **38** (2.03 eV), **44a** (0.8 eV), and **44c** (1.2 eV), and the introduction of transition-metal cations can have a marked influence, as seen for **47** (M = Cu: 1.6 eV, M = Ag: 2.2 eV) and **48** (1.4 eV).

4. Other Crystalline Chalcogen Compounds from Ionic Liquids

Aside from the hetero-polycationic chalcogenides presented above, there are a few examples of polycationic chalcogen compounds prepared in ionic liquids that do not contain chalcogen atoms in formally negative oxidation states. Ruck and co-workers isolated compounds containing Te-based polycations such as $[Mo_2Te_{12}]^{6+}$, Te_6^{2+}, and Te_4^{2+} in good

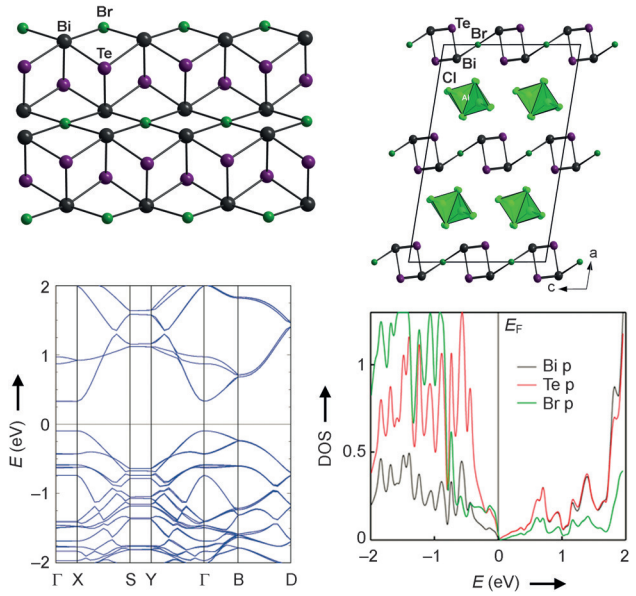

Figure 14. Top left: Fragment of the cationic 2D-$[Bi_2Te_2Br]^+$ layers within the crystal structure of **44a**. Top right: Side view of the polycationic layers in **44a** that alternate with layers containing the $[AlCl_4]^-$ anions. Bottom left: Electronic band structure of **44a**. Bottom right: Projected density of states for the p orbital of the individual elements (Bi, Te, and Br) in **44a**. Reproduced from Ref. [31b] with permission from the American Chemical Society.

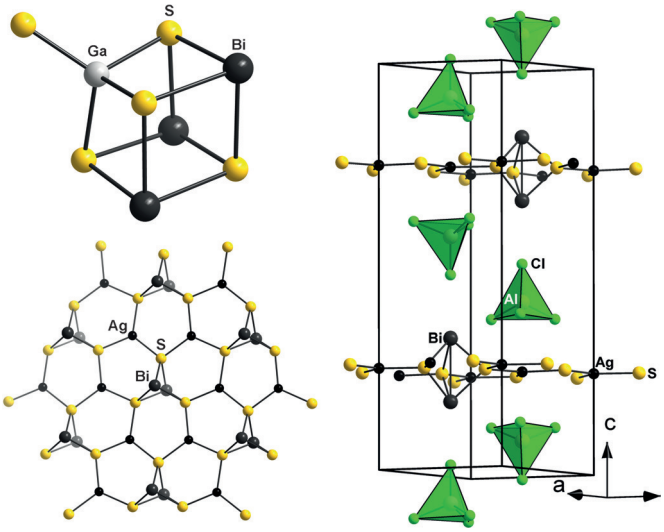

Figure 15. Top left: $[Bi_3GaS_5]^+$ cation in **46**. Bottom left: Fragment of one polycationic 2D-$[M_2Bi_2S_3]^{2+}$ layer within the crystal structure of **47**. Right: Alternating packing of polycationic layers and the $[AlCl_4]^-$ counterions in the crystal structure of **47**.

yield from room-temperature reactions in ionic liquids.[63] This stands in contrast to earlier syntheses of these or similar compounds, which required high temperatures and long reaction times.

The groups of Beck and Ruck demonstrated that two closely related polycationic tellurium compounds, $Te_4[Bi_{0.67}Cl_4]$ (**49a**) and $Te_4[Bi_{0.74}Cl_4]$ (**49b**), can be obtained

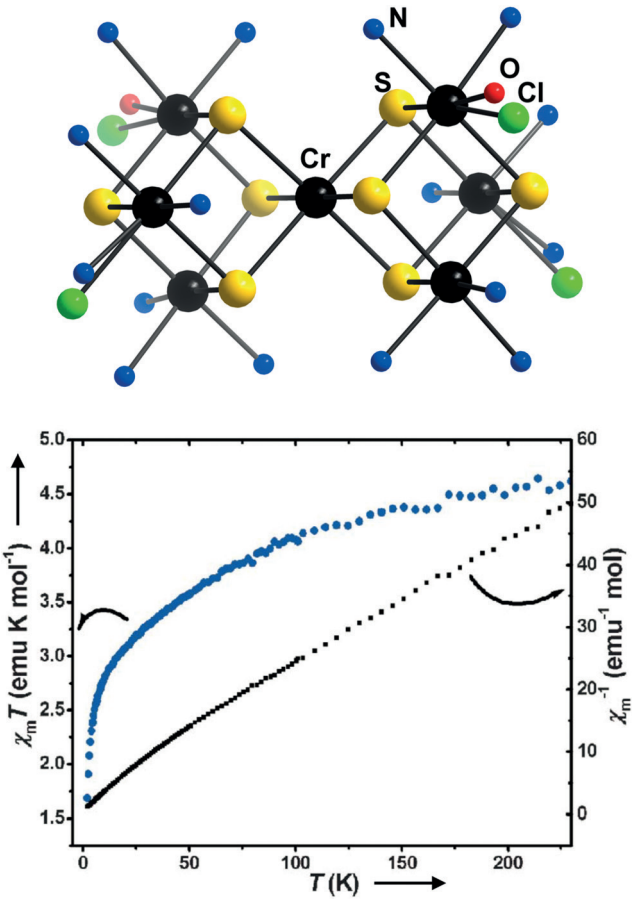

Figure 16. Top: The $[Cr_7S_8Cl_2(NH_3)_{14.5}(H_2O)_{1.5}]^{3+}$ cation in **48**. Bottom: Plots of the temperature dependence of X_mT and X_m^{-1} for **48**. Reproduced from Ref. [61] with permission from the Royal Society of Chemistry.

either from chemical vapor transport (**49a**) or from a room-temperature ionic liquid (**49b**).[64] Gold-colored needles of **49b** were synthesized using Te, $TeCl_4$, and $BiCl_3$ as starting materials in an ionic liquid composed of $[C_4C_1im]Cl$ and $AlCl_3$. **49b** is a one-dimensional metal at room temperature and a superconductor below 7.15 K. The 1D-$Te_4^{1.78+}$ cation is composed of Te_4 rings stacked into a polymeric strand (Figure 17).

Interestingly, **49a** contains the electron-precise Te_4^{2+} cation and is a semiconductor. The electronic structure of both compounds has been investigated in detail by quantum chemical methods. Figure 18 shows a part of the results, outlining the differences between the equilibrium structures and the highest occupied states of Te_4^{2+} and a hypothetical Te_4^+ cation as a product of a full one-electron reduction of Te_4^{2+}. The situation in $Te_4^{1.78+}$ is located between the two extremes.

A related kind of chemistry was presented by Krossing and co-workers. A combination of salts of weakly coordinating anions, such as $[Al(OR_F)_4]^-$ ($R_F = C(CF_3)_3$), was used in regular solvents to synthesize metal complexes containing neutral chalcogen ligands, for example, $[Ag_2Se_{12}][Al(OR_F)_4]_2$.[65]

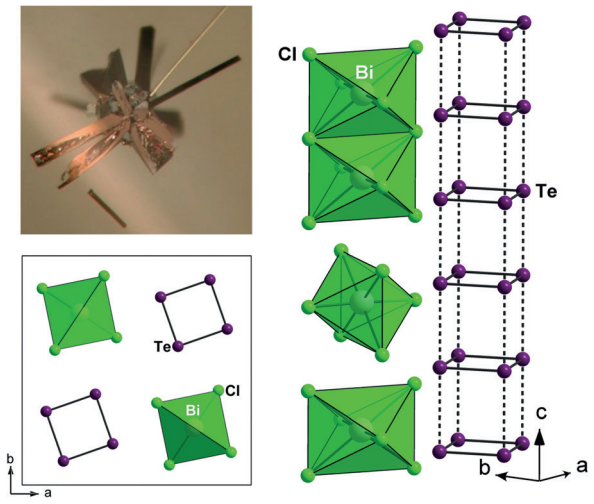

Figure 17. Top left: Photograph of the gold-colored needles of **49a**. Bottom left: Fragment of the crystal structure of **49b** viewed along the crystallographic *c*-axis. Right: A sequence of chloridobismuthate anions together with a stack of the tellurium polycation 1D-$Te_4^{1.78+}$. Reproduced from Ref. [64] with permission from Wiley-VCH.

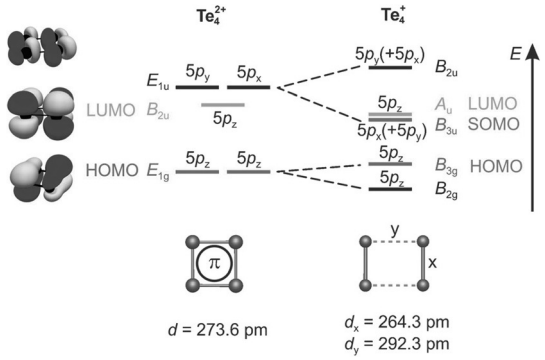

Figure 18. Semiquantitative molecular orbital schemes of the highest occupied states in the square Te_4^{2+} polycation in **49a** and the equilibrium structure of hypothetical Te_4^{+}. Reproduced from Ref. [64] with permission from Wiley-VCH.

5. Summary and Outlook

In this Review, we have summarized all the chalcogen compounds that have been obtained in single-crystalline form from ionic liquids, most of them by ionothermal techniques. Many of the products possess typical bandgaps of (photo-)semiconductors, the trend of which correlates with the dimensionality and composition along related series of compounds. In some cases, additional materials properties were reported, such as nonlinear optical media or particular reactivity. However, as the application of ionic liquids for the generation of chalcogenides is still in its infancy, the collection gives an impression about both the different synthetic approaches and the diversity and structural richness of the obtained products rather than explaining clear relationships between the chosen reaction parameters and the nature of the product. Possible future directions include the use of new elemental combinations, different ionic liquids, and further variations of the reaction conditions with guidance from, and combination with, solid-state or molten salt synthesis routes. Further work will also be dedicated to notoriously difficult mechanistic and speciation studies, to find systematic correlations that might eventually lead to the directed formation of interesting materials with fine-tunable optoelectronic and/or chemical properties.

6. Abbreviations

AD	$[M_4E_{10}]$ adamantane unit
aep	aminoethylpiperazine
d-AD	$[M_3E_9]$ defect-adamantane unit
d-HC	$[M_3E_4]$ defect-heterocubane unit
dd-HC	$[M_6E_{10}]$ double-defect-heterocubane unit
$(d\text{-HC})_C$	aggregation of d-HC into chains
$(d\text{-HC})_{DC}$	aggregation of d-HC into double chains
$(d\text{-HC})_{2D\text{-reg}}$	aggregation of d-HC into layers composed of regular six-membered rings
$(d\text{-HC})_{2D\text{-dis}}$	aggregation of d-HC into layers composed of distorted six-membered rings
$(d\text{-HC})_{2D\text{-heart}}$	aggregation of d-HC into layers composed of heart-shaped rings
$(d\text{-HC})_{2D\text{-mix}}$	aggregation of d-HC into mixed layers composed of distorted and heart-shaped rings
DABCO	diazabicyclo[2.2.2]octan
DFG	difference-frequency generation
dien	diethylenetriamine
DMMP	2,6-dimethylmorpholine
DOS	density of states
E	chalcogen
E_{ee}	electronic excitation energy
EDX	energy-dispersive X-ray spectroscopy
ELI-D	electron localizability indicator
en	ethylenediamine
en-Me	monomethylethylenediamine
HC	heterocubane unit
HH	hydrazine hydrate, $N_2H_4{\cdot}H_2O$
ICP-AES	inductively coupled plasma atomic emission spectroscopy
IL	ionic liquid
M	metal
ma	methylamine
P1	first member of the P*n* supertetrahedral family
PEG-400	poly(ethylene glycol)-400
peha	pentaethylenehexamine
PVP	poly(vinyl pyrrolidone)
SBU	secondary building unit
SC-SC	single crystal to single crystal
SHG	second harmonic generation
T	main-group (semi-)metal
T5	fifth member of the T*n* supertetrahedral family
TBU	tertiary building unit
TD	$[ME_4]$ tetrahedral unit
tepa	tetraethylenepentamine
TGA	thermogravimetric analysis
tmdp	4,4′-trimethylenedipiperidine

Acknowledgements

This work was financially supported by the Deutsche Forschungsgemeinschaft, in particular within the frameworks of the priority programs SPP1415 and SPP1708, by the Alexander von Humboldt Stiftung, and by the Friedrich Ebert Stiftung.

How to cite: *Angew. Chem. Int. Ed.* **2016**, *55*, 876 – 893
Angew. Chem. **2016**, *128*, 886 – 904

[1] a) M. Afzaal, M. A. Malik, P. O'Brien, *J. Mater. Chem.* **2010**, *20*, 4031 – 4040; b) V. V. Brazhkin, Y. Katayama, M. Kanzaki, M. V. Kondrin, A. G. Lyapin, *JETP Lett.* **2011**, *94*, 161 – 170; c) A. Mrotzek, M. G. Kanatzidis, *Acc. Chem. Res.* **2003**, *36*, 111 – 119; d) K. F. Hsu, S. Loo, F. Guo, W. Chen, J. S. Dyck, C. Uher, T. Hogan, E. K. Polychroniadis, M. G. Kanatzidis, *Science* **2004**, *303*, 818 – 821; e) I. U. Arachchige, J. Wu, V. P. Dravid, M. G. Kanatzidis, *Adv. Mater.* **2008**, *20*, 3638 – 3642; f) J. L. Mohanan, I. U. Arachchige, S. L. Brock, *Science* **2005**, *307*, 397 – 400; g) N. Kamaya, K. Homma, Y. Yamakawa, M. Hirayama, R. Kanno, M. Yonemura, T. Kamiyama, Y. Kato, S. Hama, K. Kawamoto, A. Mitsui, *Nat. Mater.* **2011**, *10*, 682 – 686; h) P. Bron, S. Johansson, K. Zick, J. Schmedt auf der Günne, S. Dehnen, B. Roling, *J. Am. Chem. Soc.* **2013**, *135*, 15694 – 15697.

[2] a) N. Zheng, X. Bu, P. Feng, *Nature* **2003**, *426*, 428 – 432; b) N. Zheng, X. Bu, H. Vu, P. Feng, *Angew. Chem. Int. Ed.* **2005**, *44*, 5299 – 5303; *Angew. Chem.* **2005**, *117*, 5433 – 5437.

[3] a) P. Feng, X. Bu, N. Zheng, *Acc. Chem. Res.* **2005**, *38*, 293 – 303; b) N. Zheng, X. Bu, B. Wang, P. Feng, *Science* **2002**, *298*, 2366 – 2369.

[4] a) P. Vaqueiro, *Dalton Trans.* **2010**, *39*, 5965 – 5972; b) S. Dehnen, M. Melullis, *Coord. Chem. Rev.* **2007**, *251*, 1259 – 1280; c) X. Bu, N. Zheng, P. Feng, *Chem. Eur. J.* **2004**, *10*, 3356 – 3362; d) W. S. Sheldrick, M. Wachhold, *Coord. Chem. Rev.* **1998**, *176*, 211 – 322; e) C. L. Bowes, G. A. Ozin, *Adv. Mater.* **1996**, *8*, 13 – 28.

[5] a) N. Zheng, X. Bu, P. Feng, *J. Am. Chem. Soc.* **2003**, *125*, 1138 – 1139.

[6] a) Z. Zhang, J. Zhang, T. Wu, X. Bu, P. Feng, *J. Am. Chem. Soc.* **2008**, *130*, 15238 – 15239; b) Y. Liu, P. D. Kanhere, C. L. Wong, Y. Tian, Y. Feng, F. Boey, T. Wu, H. Chen, T. J. White, Z. Chen, Q. Zhang, *J. Solid State Chem.* **2010**, *183*, 2644 – 2649; c) K.-Y. Wang, M.-L. Feng, D.-N. Kong, S.-J. Liang, L. Wu, X.-Y. Huang, *CrystEngComm* **2012**, *14*, 90 – 94.

[7] S. Haddadpour, M. Mellullis, H. Staesche, C. R. Mariappan, B. Roling, R. Clérac, S. Dehnen, *Inorg. Chem.* **2009**, *48*, 1689 – 1698.

[8] a) N. Ding, M. G. Kanatzidis, *Nat. Chem.* **2010**, *2*, 187 – 191; b) M.-L. Feng, D.-N. Kong, Z.-L. Xie, X.-Y. Huang, *Angew. Chem. Int. Ed.* **2008**, *47*, 8623 – 8626; *Angew. Chem.* **2008**, *120*, 8751 – 8754; c) M. J. Manos, C. D. Malliakas, M. G. Kanatzidis, *Chem. Eur. J.* **2007**, *13*, 51 – 58; d) M. J. Manos, K. Chrissafis, M. G. Kanatzidis, *J. Am. Chem. Soc.* **2006**, *128*, 8875 – 8883; e) M. J. Manos, R. G. Iyer, E. Quarez, J. H. Liao, M. G. Kanatzidis, *Angew. Chem. Int. Ed.* **2005**, *44*, 3552 – 3555; *Angew. Chem.* **2005**, *117*, 3618 – 3621; f) H. Li, A. Laine, M. O'Keeffe, O. M. Yaghi, *Science* **1999**, *283*, 1145 – 1147; g) T. J. McCarthy, T. A. Tanzer, M. G. Kanatzidis, *J. Am. Chem. Soc.* **1995**, *117*, 1294 – 1301.

[9] a) D. Freudenmann, S. Wolf, M. Wolff, C. Feldmann, *Angew. Chem. Int. Ed.* **2011**, *50*, 11050 – 11060; *Angew. Chem.* **2011**, *123*, 11244 – 11255; b) S. J. Mugavero, M. Bharathy, J. McAlum, H. C. zur Loye, *Solid-State Sci.* **2008**, *10*, 370 – 376.

[10] a) M. G. Kanatzidis, *Chem. Mater.* **1990**, *2*, 353 – 363; b) M. G. Kanatzidis, A. C. Sutorik, *Prog. Inorg. Chem.* **1995**, *43*, 151 – 265; c) S. Johnsen, S. C. Peter, S. L. Nguyen, J.-H. Song, H. Jin, A. J. Freeman, M. G. Kanatzidis, *Chem. Mater.* **2011**, *23*, 4375 – 4383.

[11] E. R. Cooper, C. D. Andrews, P. S. Wheatley, P. B. Webb, P. Wormald, R. E. Morris, *Nature* **2004**, *430*, 1012 – 1016.

[12] a) W. S. Sheldrick, *Dalton Trans.* **2000**, 3041 – 3052; b) T. Jiang, G. A. Ozin, *J. Mater. Chem.* **1998**, *8*, 1099 – 1108.

[13] a) T. Wu, X. Bu, X. Zhao, R. Khazhakyan, P. Feng, *J. Am. Chem. Soc.* **2011**, *133*, 9616 – 9625; b) T. Wu, X. Wang, X. Bu, X. Zhao, L. Wang, P. Feng, *Angew. Chem. Int. Ed.* **2009**, *48*, 7204 – 7207; *Angew. Chem.* **2009**, *121*, 7340 – 7343.

[14] a) L. Iordanidis, M. G. Kanatzidis, *J. Am. Chem. Soc.* **2000**, *122*, 8319 – 8320; b) T. Wu, L. Wang, X. Bu, V. Chau, P. Feng, *J. Am. Chem. Soc.* **2010**, *132*, 10823 – 10831; c) H. Ahari, A. Lough, S. Petrov, G. A. Ozin, R. L. Bedard, *J. Mater. Chem.* **1999**, *9*, 1263 – 1274.

[15] a) Z.-M. Hao, X.-M. Zhang, *Dalton Trans.* **2011**, *40*, 2092 – 2098; b) G. S. Papaefstathiou, Z. Zhong, L. Geng, L. R. MaGillivray, *J. Am. Chem. Soc.* **2004**, *126*, 9158 – 9159; c) T. Haneda, M. Kawano, T. Kawamichi, M. Fujita, *J. Am. Chem. Soc.* **2008**, *130*, 1578 – 1579; d) Y.-F. Han, W.-G. Jia, Y.-J. Lin, G.-X. Jin, *Angew. Chem. Int. Ed.* **2009**, *48*, 6234 – 6238; *Angew. Chem.* **2009**, *121*, 6352 – 6356; e) E. Y. Lee, M. P. Suh, *Angew. Chem. Int. Ed.* **2004**, *43*, 2798 – 2801; *Angew. Chem.* **2004**, *116*, 2858 – 2861; f) N. L. Toh, M. Nagarathinam, J. Vittal, *Angew. Chem. Int. Ed.* **2005**, *44*, 2237 – 2241; *Angew. Chem.* **2005**, *117*, 2277 – 2281; g) Q. Chu, D. C. Swenson, L. R. MacGillivray, *Angew. Chem. Int. Ed.* **2005**, *44*, 3569 – 3572; *Angew. Chem.* **2005**, *117*, 3635 – 3638.

[16] a) J. W. Lauher, F. W. Fowler, N. S. Goroff, *Acc. Chem. Res.* **2008**, *41*, 1215 – 1229; b) J.-P. Zhang, Y.-Y. Lin, W.-X. Zhang, X.-M. Chen, *J. Am. Chem. Soc.* **2005**, *127*, 14162 – 14163; c) T. Friščić, L. R. MacGillivray, *Z. Kristallogr.* **2005**, *220*, 351 – 363.

[17] J. Heine, S. Dehnen, *Z. Anorg. Allg. Chem.* **2012**, *638*, 2425 – 2440.

[18] W.-W. Xiong, Q. Zhang, *Angew. Chem. Int. Ed.* **2015**, *54*, 11616 – 11623; *Angew. Chem.* **2015**, *127*, 11780 – 11788.

[19] W.-W. Xiong, E. U. Athresh, Y. T. Ng, J. Ding, T. Wu, Q. Zhang, *J. Am. Chem. Soc.* **2013**, *135*, 1256 – 1259.

[20] J. Gao, Q. Tay, P.-Z. Li, W.-W. Xiong, Y. Zhao, Z. Chen, Q. Zhang, *Chem. Asian J.* **2014**, *9*, 131 – 134.

[21] G. A. Alanko, D. P. Butt, *J. Am. Ceram. Soc.* **2014**, *97*, 2357 – 2359.

[22] a) P. Wasserscheid, T. Welton, *Ionic Liquids in Synthesis*, Wiley-VCH, Weinheim, **2008**; b) R. Giernoth, *Angew. Chem. Int. Ed.* **2010**, *49*, 2834 – 2839; *Angew. Chem.* **2010**, *122*, 2896 – 2901; c) Z. Ma, J. Yu, S. Dai, *Adv. Mater.* **2010**, *22*, 261 – 285.

[23] P. Walden, *Izv. Imp. Akad. Nauk* **1914**, 405 – 422.

[24] a) E. F. Aust, *Nachr. Chem.* **2009**, *156*, 529 – 530; b) S. Werner, M. Haumann, P. Wasserscheid, *Annu. Rev. Chem. Biomol. Eng.* **2010**, *1*, 203 – 230; c) L. F. Vega, O. Vilaseca, F. Llovell, *Fluid Phase Equilib.* **2010**, *294*, 15 – 30.

[25] a) Z. B. Zhou, H. Matsumoto, K. Tatsumi, *Chem. Eur. J.* **2006**, *12*, 2196 – 2212; b) I. Krossing, J. M. Slattery, C. Daguenet, P. J. Dyson, *J. Am. Chem. Soc.* **2006**, *128*, 13427 – 13434; c) D. Zahn, F. Uhlig, J. Thar, C. Spickermann, B. Kirchner, *Angew. Chem. Int. Ed.* **2008**, *47*, 3639 – 3641; *Angew. Chem.* **2008**, *120*, 3695 – 3697; d) P. Hapiot, C. Lagrost, *Chem. Rev.* **2008**, *108*, 2238 – 2264; e) K. Ueno, H. Tokuda, M. Watanabe, *Phys. Chem. Chem. Phys.* **2010**, *12*, 1649 – 1658; f) D. Rooney, J. Jacquemin, R. Gardas, *Top. Curr. Chem.* **2009**, *290*, 185 – 212; g) S. Aparicio, M. Atilhan, F. Karadas, *Ind. Eng. Chem. Res.* **2010**, *49*, 9580 – 9595; h) P. M. Dean, J. M. Pringle, D. R. MacFarlane, *Phys. Chem. Chem. Phys.* **2010**, *12*, 9144 – 9153.

[26] H. Niedermeyer, J. P. Hallett, I. J. Villar-Garcia, P. A. Hunt, T. Welton, *Chem. Soc. Rev.* **2012**, *41*, 7780 – 7802.

[27] R. E. Morris, *Chem. Commun.* **2009**, 2990 – 2998.

[28] R. E. Morris, *Dalton Trans.* **2012**, *41*, 3867 – 3868.

[29] Z. Lin, D. S. Wragg, J. E. Warren, R. E. Morris, *J. Am. Chem. Soc.* **2007**, *129*, 10334 – 10335.

[30] A. M. Guloy, R. Ramlau, Z. Tang, W. Schnelle, M. Baitinger, Y. Grin, *Nature* **2006**, *443*, 320 – 323.
[31] a) Q. Zhang, I. Chung, J. I. Jang, J. B. Ketterson, M. G. Kanatzidis, *J. Am. Chem. Soc.* **2009**, *131*, 9896 – 9897; b) K. Biswas, Q. Zhang, I. Chung, J.-H. Song, J. Androulakis, A. J. Freeman, M. G. Kanatzidis, *J. Am. Chem. Soc.* **2010**, *132*, 14760 – 14762; c) J. R. Li, Z.-L. Xie, X.-W. He, L.-H. Li, X.-Y. Huang, *Angew. Chem. Int. Ed.* **2011**, *50*, 11395 – 11399; *Angew. Chem.* **2011**, *123*, 11597 – 11601.
[32] W. S. Sheldrick, M. Wachhold, *Angew. Chem. Int. Ed. Engl.* **1997**, *36*, 206 – 224; *Angew. Chem.* **1997**, *109*, 214 – 234.
[33] J.-R. Li, W.-W. Xiong, Z.-L. Xie, C.-F. Du, G.-D. Zou, X.-Y. Huang, *Chem. Commun.* **2013**, *49*, 181 – 183.
[34] a) A. Loose, *Dissertation*, Universität Bochum **1998**; b) J. Zhou, G. Bian, Y. Zhang, A. Tang, Q. Zu, *Inorg. Chem.* **2007**, *46*, 1541 – 1543; c) W. S. Sheldrick, B. Schaaf, *Z. Anorg. Allg. Chem.* **1994**, *620*, 1041 – 1045; d) W. S. Sheldrick, H. G. Braunbeck, *Z. Anorg. Allg. Chem.* **1993**, *619*, 1300 – 1306; e) H. Ahari, C. L. Bowes, T. Jiang, A. Lough, G. A. Ozin, R. L. Bedard, S. Petrov, D. Young, *Adv. Mater.* **1995**, *7*, 375 – 378; f) W. S. Sheldrick, H. G. Braunbeck, *Z. Naturforsch. B* **1990**, *45*, 1643 – 1646; g) J. B. Parise, Y. Ko, J. Rijssenbeck, D. M. Nellis, K. Tan, S. Koch, *J. Chem. Soc. Chem. Commun.* **1994**, 527; h) T. Jiang, A. Lough, G. A. Ozin, *Adv. Mater.* **1998**, *10*, 42 – 46.
[35] G. Xu, C. Wang, P. Guo, *Acta Crystallogr. Sect. C* **2009**, *65*, m17 – m173.
[36] C.-F. Du, J.-R. Li, M.-L. Feng, G.-D. Zou, N.-N. Shen, X.-Y. Huang, *Dalton Trans.* **2015**, *44*, 7364 – 7372.
[37] H. Sakamoto, Y. Watanabe, T. Saito, *Inorg. Chem.* **2006**, *45*, 4578 – 4579.
[38] J. A. Cody, K. B. Finch, G. J. Reynders III, G. C. B. Alexander, H. G. Lim, C. Näther, W. Bensch, *Inorg. Chem.* **2012**, *51*, 13357 – 13362.
[39] W.-W. Xiong, J.-R. Li, B. Hu, B. Tan, R.-F. Li, X.-Y. Huang, *Chem. Sci.* **2012**, *3*, 1200 – 1204.
[40] T. Wu, X. Bu, P. Liao, L. Wang, S.-T. Zheng, R. Ma, P. Feng, *J. Am. Chem. Soc.* **2012**, *134*, 3619 – 3622.
[41] X. H. Bu, N. F. Zheng, Y. Q. Li, P. Y. Feng, *J. Am. Chem. Soc.* **2002**, *124*, 12646 – 12647.
[42] G. Thiele, S. Santner, C. Donsbach, M. Assmann, M. Müller, S. Dehnen, *Z. Kristallogr.* **2014**, *229*, 489 – 495.
[43] J.-L. Lu, C.-Y. Tang, F. Wang, Y.-L. Shen, Y.-X. Yuan, D.-X. Jia, *Inorg. Chem. Commun.* **2014**, *47*, 148 – 151.
[44] Y. Lin, W. Massa, S. Dehnen, *J. Am. Chem. Soc.* **2012**, *134*, 4497 – 4500.
[45] a) L. Wang, Y. P. Xu, Y. Wei, J. C. Duan, A. B. Chen, B. C. Wang, H. J. Ma, Z. J. Tian, L. W. Lin, *J. Am. Chem. Soc.* **2006**, *128*, 7432 – 7433; b) R. S. Xu, W. P. Zhang, J. Guan, Y. P. Xu, L. Wang, H. J. Ma, Z. J. Tian, X. W. Han, L. W. Lin, X. H. Bao, *Chem. Eur. J.* **2009**, *15*, 5348 – 5354.
[46] Y. Lin, S. Dehnen, *Inorg. Chem.* **2011**, *50*, 7913 – 7915.
[47] Y. Lin, W. Massa, S. Dehnen, *Chem. Eur. J.* **2012**, *18*, 13427 – 13434.
[48] a) O. M. Yaghi, Z. Sun, D. A. Richardson, T. L. Groy, *J. Am. Chem. Soc.* **1994**, *116*, 807 – 808; b) C. L. Bowes, A. J. Lough, A. Malek, G. A. Ozin, S. Petrov, D. Young, *Chem. Ber.* **1996**, *129*, 283 – 287; c) C. L. Bowes, W. U. Huynh, S. J. Kirkby, A. Malek, G. A. Ozin, S. Petrov, M. Twardowski, D. Young, R. L. Bedard, R. Broach, *Chem. Mater.* **1996**, *8*, 2147 – 2152; d) H. Ahari, A. Garcia, S. Kirkby, G. A. Ozin, D. Young, A. J. Lough, *J. Chem. Soc. Dalton Trans.* **1998**, 2023 – 2027; e) A. Loose, W. S. Sheldrick, *Z. Naturforsch. B* **1997**, *52*, 687 – 692.
[49] S. Santner, S. Dehnen, *Inorg. Chem.* **2015**, *54*, 1188 – 1190.
[50] K. O. Klepp, *Z. Naturforsch. B* **1992**, *47*, 197 – 200.
[51] Y. Lin, D. Xie, W. Massa, L. Mayrhofer, S. Lippert, B. Ewers, A. Chernikov, M. Koch, S. Dehnen, *Chem. Eur. J.* **2013**, *19*, 8806 – 8813.
[52] J. S. Wilkes, *Green Chem.* **2002**, *4*, 73 – 80.
[53] a) J. Beck, *Coord. Chem. Rev.* **1997**, *163*, 55 – 70; b) S. Brownridge, I. Krossing,, J. Passmore, H. D. B. Jenkins, H. K. RooUnten, *Coord. Chem. Rev.* **2000**, *197*, 397 – 481; c) I. Krossing in *Molecular Clusters of the Main Group Elements* (Eds.: M. Driess, H. Nöth), Wiley-VCH, Weinheim, **2004**, pp. 209 – 229; d) W. S. Sheldrick in *Molecular Clusters of the Main Group Elements* (Eds.: M. Driess, H. Nöth), Wiley-VCH, Weinheim, **2004**, pp. 230 – 245; e) E. Ahmeda, M. Rucka, *Coord. Chem. Rev.* **2011**, *255*, 2892 – 2903; f) T. A. Engesser, I. Krossing, *Coord. Chem. Rev.* **2013**, *257*, 946 – 955.
[54] E. Ahmed, A. Isaeva, A. Fiedler, M. Haft, M. Ruck, *Chem. Eur. J.* **2011**, *17*, 6847 – 6852.
[55] E. Ahmed, J. Breternitz, M. F. Groh, A. Isaeva, M. Ruck, *Eur. J. Inorg. Chem.* **2014**, 3037 – 3042.
[56] a) M. Kohout, *Faraday Discuss.* **2007**, *135*, 43 – 54; b) M. Kohout, *Int. J. Quantum Chem.* **2004**, *97*, 651 – 658.
[57] M. F. Groh, J. Breternitz, E. Ahmed, A. Isaeva, A. Efimova, P. Schmidt, M. Ruck, *Z. Anorg. Allg. Chem.* **2015**, *641*, 388 – 393.
[58] K. Biswas, I. Chung, J.-Hw. Song, C. D. Malliakas, A. J. Freeman, M. G. Kanatzidis, *Inorg. Chem.* **2013**, *52*, 5657 – 5659.
[59] D. Freudenmann, C. Feldmann, *Dalton Trans.* **2011**, *40*, 452 – 456.
[60] M. F. Groh, M. Knies, A. Isaeva, M. Ruck, *Z. Anorg. Allg. Chem.* **2015**, *641*, 279 – 284.
[61] K.-Z. Du, M.-L. Feng, J.-R. Li, X.-Y. Huang, *CrystEngComm* **2013**, *15*, 5594 – 5597.
[62] a) J. Beck, M. Dolg, S. Schlüter, *Angew. Chem. Int. Ed.* **2001**, *40*, 2287 – 2290; *Angew. Chem.* **2001**, *113*, 2347 – 2350; b) A. Eich, W. Hoffbauer, G. Schnakenburg, T. Bredow, J. Daniels, J. Beck, *Eur. J. Inorg. Chem.* **2014**, 3043 – 3052; c) A. Eich, T. Bredow, J. Beck, *Inorg. Chem.* **2015**, *54*, 484 – 491.
[63] E. Ahmed, E. Ahrens, M. Heise, M. Ruck, *Z. Anorg. Allg. Chem.* **2010**, *636*, 2602 – 2606.
[64] E. Ahmed, J. Beck, J. Daniels, T. Doert, S. Jan Eck, A. Heerwig, A. Isaeva, S. Lidin, M. Ruck, W. Schnelle, A. Stankowski, *Angew. Chem. Int. Ed.* **2012**, *51*, 8106 – 8109; *Angew. Chem.* **2012**, *124*, 8230 – 8233.
[65] a) G. Santiso-Quiñones, A. Higelin, J. Schaefer, R. Brückner, C. Knapp, I. Krossing, *Chem. Eur. J.* **2009**, *15*, 6663 – 6677; b) G. Santiso-Quiñones, R. Brückner, C. Knapp, I. Dionne, J. Passmore, I. Krossing, *Angew. Chem. Int. Ed.* **2009**, *48*, 1133 – 1137; *Angew. Chem.* **2009**, *121*, 1153 – 1157; c) T. Köchner, N. Trapp, T. A. Engesser, A. J. Lehner, C. Röhr, S. Riedel, C. Knapp, H. Scherer, I. Krossing, *Angew. Chem. Int. Ed.* **2011**, *50*, 11253 – 11256; *Angew. Chem.* **2011**, *123*, 11449 – 11452.

Received: August 18, 2015
Published online: December 11, 2015

